

COMBUSTION OF A SINGLE FUEL DROPLET
IN AN OXIDIZING ATMOSPHERE

Z. A. SIDDIQI

A DISSERTATION
IN
THE FACULTY
OF
ENGINEERING

PRESENTED IN PARTIAL FULFILLMENT OF
THE REQUIREMENT FOR THE DEGREE OF
MASTER OF ENGINEERING AT
CONCORDIA UNIVERSITY
MONTREAL, QUEBEC, CANADA

March 1980

© Z. A. Siddiqi, 1980

ABSTRACT

ABSTRACT

COMBUSTION OF A SINGLE FUEL DROPLET
IN AN OXIDIZING ATMOSPHERE

ZAFAR A. SIDDIQI

Combustion of a single fuel droplet in an oxidizing atmosphere has been reviewed. Various problems associated with the droplet combustion have been critically examined. Attempts have been made to establish the parameters which could predict realistic behaviour of the combustion of a single droplet. Present combustion theories predict d^2 law accurately over a wide range and a burning constant can be realistically predicted by these theories. This study establishes that the burning rate is independent of the flame temperature and the position of the flame. Moreover, the burning constant can be predicted accurately by the use of quasi-steady state theory provided the variation of the thermal conductivity and specific heat with temperature is taken into account. The flame temperature can be realistically estimated by including the effect of radiation based on the actual condition of the flame, and the ratio of the flame diameter to drop diameters can be determined by taking into account the convection, radiation effect and the transfer properties.

ACKNOWLEDGEMENTS

ACKNOWLEDGEMENT

The author expresses his sincere appreciation to Dr. S. Lin of the Mechanical Engineering Department of Concordia University for his guidance and advice with preparation of this dissertation.

TABLE OF CONTENTS

TABLE OF CONTENTS

	<u>PAGE</u>
ABSTRACT	(i)
ACKNOWLEDGEMENTS	(ii)
LIST OF TABLES	(v)
LIST OF FIGURES	(vi)
NOMENCLATURE	(vii)
 <u>CHAPTER 1</u>	
INTRODUCTION	1
1.1 General	1
1.2 Scope of Study	3
 <u>CHAPTER 2</u>	
COMBUSTION IN STAGNANT SURROUNDING	4
2.1 General	4
2.2 Steady State	5
2.3 Unsteady Effects	10
2.4 Kinetic Effects	15
2.5 Oxygen/Fuel Ratio	16
 <u>CHAPTER 3</u>	
EFFECT OF VARIABLE PROPERTIES IN COMBUSTION	17
3.1 Review of the Existing Work	17
3.2 Calculation of the Parameters Affecting the Combustion of the Droplet	19
 <u>CHAPTER 4</u>	
COMBUSTION IN CONVECTIVE GAS FLOW	23
4.1 General	23
4.2 With Natural Convection Effects	24
4.3 With Forced Convection Effects	24

TABLE OF CONTENTS (Cont'd)

	<u>PAGE</u>
<u>CHAPTER 5</u>	
HEAT TRANSFER BY RADIATION TO A FUEL DROPLET	28
5.1 General	28
5.2 Emmissivity	29
5.3 Absorption	31
<u>CHAPTER 6</u>	
HEAT AND MASS TRANSFER FROM DROPS	34
<u>CHAPTER 7</u>	
DISCUSSION	35
7.1 General	35
7.2 Mass Burning Rate	36
7.3 The Ratio of Flame Diameter/Drop Diameter	39
7.4 Flame Temperature	39
<u>CHAPTER 8</u>	
CONCLUSION	41
TABLES	42
FIGURES	51
REFERENCES	65
<u>APPENDIX A</u>	
METHOD OF CALCULATING DRAG CO-EFFICIENTS FOR THE COMBUSTION OF A DROPLET IN FORCED CONVECTIVE EFFECT	73
<u>APPENDIX B</u>	
COMPUTER PRINT-OUT OF THE THERMODYNAMIC AND TRANSPORT PROPERTIES FOR BENZENE	79

LIST OF TABLES

LIST OF TABLES

<u>TABLE</u>	<u>DESCRIPTION</u>	<u>PAGE</u>
1.	Burning Constants for Various Hydrocarbons (oxidant at 20°C and 1 atmosphere)	42
2.	A General Comparison of Experimental Data With Quasi-Steady State Prediction (Material: n heptane)	43
3.	Comparison of Combustion Parameters for Benzene Droplet of 2mm in Analysis With Constant k and Variable Thermodynamic Properties	44
4.	Comparison of Combustion Parameters for Benzene Droplet of 2 mm in Analysis With Variable k and Thermodynamic Properties	45
5.	The Effects of Ambient Gas Velocity on the Burning Constant	46
6.	Various Correlation of the Mass Burning Rate or Mass Rate of Evaporation Under Forced Convection Condition	47
7.	Constant for Calculating Total Absorption of 1000°C Radiation by Heavy Fuel Oil	49
8.	Value of "B" in Air	50

LIST OF FIGURES

LIST OF FIGURES

<u>FIGURES</u>	<u>DESCRIPTION</u>	<u>PAGE</u>
1.	Spherically Symmetrical Model of a Burning Droplet	51
2.	Flame Temperature for Various Common Hydrocarbon Liquid Fuel	52
3.	Comparison of d_p^2 Vs t Curves in Ref. [44] With Experimental Results Ref. [38, 43]	53
4.	Variation of Specific Heat (C_p) With Temperature for Benzene	54
5.	Dependence of $\frac{d_f}{d_l}$ and m/r_L on b_1 in the Analysis of Goldsmith and Penner	55
6.	Ideal Model of a Burning Droplet in Presence of Convection	56
7.	The Variation of Local Heat Transfer Rate Over a Drop Surface Under Forced Convection Conditions (after graves and Bahr [29])	57
8.	Drag Coefficient (C_D) Against Reynold's Number (Re) for the Combustion of a Droplet in Forced Convection Atmosphere	58
9.	C_{\perp} and C_{\parallel} for an Opaque Dielectric With a Refractive Index of 1.5	59
10.	Directional Emmissivity of Strong Absorbers	60
11.	Internal Local Volumetric Absorption Rate, in an Absorbing Reflecting Sphere, the Surface of Which is Uniformly Irradiated With Hemispherical Flux, Refractive Index 1.5	61
12.	Species and Temperature Profile for a Burning Droplets	62
13.	Benzene Droplet in Stagnant Air - Showing Diameter Squared Time Dependency	63
14.	Relationship of d^2 Against t for Single Droplets of Various Fuels	64

NOMENCLATURE

NOMENCLATURE

a	experimentally determined constant
a'	constant (equation 4)
A	pre-exponential factor in the rate constant (equation 18)
A _L	constants
b	experimentally determined constant
b'	constant (equation 4)
B	transfer number (equation 11)
B _{ev}	transfer number in evaporation (equation 18)
c	specific heat
C _a	specific heat of air at log mean temperature
C _d	drag coefficient
C _m	mass-concentration of particles
C _n	total number of carbon atoms in hydrocarbons
C _p -c _p	specific heat at constant pressure
C ₁ -C ₂	first and second Planck constants
C ₁ '	constant
d	droplet diameter
d _c	cenosphere diameter
d _f	flame diameter
d _l	drop diameter
d ₀	initial droplet diameter
d ₁ , d ₂	diameters of thin spherical shells
d _∞	diameter of a spherical shell at infinite distance from the drop surface
D	mean diffusivity of oxygen beyond the flame
D ₀	dimensionless diffusive oxidizer flux (equation 18)

E	activation energy
$E_{\lambda}(E_w)$	monochromatic emissive power of a black body at wave length λ (wave number w). Units-energy/(area) (time) (wave length or wave number)
$E_{\lambda g}(E_{\lambda s})$	monochromatic emissive power of a gas and surface at wave length λ respectively
f	frequency (C/S)
f_v	volume fraction of space occupied by particles
Gr	Grashoff number
H	heat of combustion
i	stoichiometric ratio
k	thermal conductivity at temperature T
k_a	thermal conductivity of air at log mean temperature
k_l	thermal conductivity of liquid
K	absorption coefficient
K_1, K_2	experimentally determined constants (equation 40)
KR	product of absorption coefficient and the radius of sphere
L	path length; distance; characterizing dimension
\dot{m}	mass burning rate
$\frac{dm}{dt}$	mass burning rate
M_f	mass rate of evaporation under forced convection conditions
M_n	mass rate of evaporation under natural convection conditions
M_s	mass rate of evaporation in absence of convection
M_{O_2}	mass fraction of oxygen in the ambient gas
n	overall order of reaction
N	real part of refractive index

N mole fraction of oxygen in bulk surrounding gas
 Nu Nusselt number
 \overline{Nu} Nusselt number in presence of mass transfer
 P pressure
 Pr Prandtl number
 $P, (P_d)$ specular (diffuse) reflectance
 P_1 amplitude of air vibration
 Q heat required to evaporate unit mass of fuel
 Q_1 heat of vaporization for the component 1
 Q_2 heat of vaporization for the component 2
 r constant mean drop radius
 r radial co-ordinate
 r_f flame radius
 r_d drop radius
 R growth rate of droplets
 R_a heat transmission by radiation
 Re Reynolds number
 R_1 universal gas constant ($82.06 \text{ cm}^3 \text{ atm/g mole } ^\circ\text{K}$)
 R_2 universal gas constant ($1.987 \text{ cal/g mole } ^\circ\text{K}$)
 t time
 t_b burning time

T absolute temperature
 T_a temperature of ambient air
 T_B reaction zone temperature
 T_f flame temperature
 T_g temperature of the ambient gas
 T_i ignition time
 T_l temperature of the liquid drop
 T_s surface temperature of the drop
 v radial velocity
 v or V volume
 V air velocity
 V_0 burning velocity
 V_{O_2} volume concentration of O_2 in the ambient gas
 X ratio of particle perimeter to wave length of incident radiation
 X number of moles of combustion products derived from stoichiometric combustion of unit mass of fuel with oxygen
 X absorptivity, absorptance
 X_d absorptivity of the drop
 $X_{gs} (X_{1,2})$ absorptivity of a gas for radiation from a surface (of surface 1 for radiation from 2).
 Y_0 weight fraction of oxygen in air
 Y_1 weight fraction of the component 1
 Y_2 weight fraction of the component 2

Y_{oi}	mass fraction of oxidizer at the droplet surface
$Y_{x\infty}$	mole fraction of gaseous reactant at infinity fuel
Z	air ratio
O/F	oxygen-fuel ratio
α	thermal diffusivity of the liquid
α_v	thermal diffusivity of the vapour-gas mixture
ϵ_f	emissivity of the flame
ϵ_g, ϵ_s	emissivity or emittance of a gas and of a surface respectively
ϵ	equivalent plane emissivity
θ	polar angle
K	absorption index
λ	burning or evaporation constant
λ_s	burning constant with no vibrations
λ_2	burning constant with vibrations
$\bar{\lambda}$	wave length
π	constant (3.1416)
ρ	mean density of oxygen beyond the flame
ρ_l	density of the liquid
ρ_1	density of the component 1
ρ_2	density of the component 2
$\rho_{\perp}, \rho_{\parallel}$	perpendicular and parallel to plane reflectances containing beam of interest respectively
σ	Stefan - Boltzmann constant
n	number of moles of oxygen required for stoichiometric combustion of unit mass of fuel.

CHAPTER 1

INTRODUCTION

CHAPTER 1

INTRODUCTION

1.1 General

The mechanism of combustion is applicable to a variety of mechanical equipment such as gas turbines, furnaces and boilers. Such equipment can be designed for optimal use of liquid fuel which may range from light distillate to residual fuel oil.

The study of the behaviour of a single isolated droplet in the combustion process is a pre-requisite for obtaining an insight into the mechanism of this process. Such study will also provide a better understanding of the parameters governing the design of equipment for combustion processes.

Single drop combustion is the mechanism that initiates the overall combustion of the sprays and governs such parameter as ignition lag.

The core of fuel sprays is composed of drops and fuel-vapour/air mixture that are too cool and too rich due to evaporation and possible adiabatic saturation, to initiate combustion. Once ignition begins, spray vaporization and flame front combustion mechanisms take over.

Before liquid fuel can burn effectively in a combustion chamber, it must be reduced to minute droplets [12]. This is accomplished by atomizing.

1.1 General (Cont'd)

The fuel is thus introduced into the combustion chamber in the form of a spray of droplets with a certain velocity distribution.

The main purpose of atomization is to increase the surface area of the liquid interface to intensify vapourization, to obtain good distribution of the fuel in the chamber and to ensure easier access of the oxidant to the vapour of the droplets [6].

Following atomization, combustion then takes place through a series of complex processes, most of which are only incompletely understood. The most important steps in this process are: [32, 54].

- a) Mixing of the droplets with air and hot combustion products - a process usually occurring under turbulent conditions.
- b) Transfer of heat to the droplets by convection from the preheated oxidant and recycled combustion gases and radiation from the flame and chamber walls.
- c) Evaporation of the droplets, often accompanied by cracking of the vapour.
- d) Mixing of the vapour with air and combustion gases to form an inflammable mixture.
- e) Ignition of the gaseous mixture. Depending on the mixing conditions, a diffusion flame may either occur at the oxygen-rich boundaries of eddies containing many vapourizing droplets or individual droplets which may be wholly or partly surrounded by their own small flames. Transition from one mechanism to the other can occur along the flame path in the furnace.

1.2 Scope of the Study

This dissertation deals with the combustion of a single isolated droplet. This study has been carried out with the main object of ascertaining the relative importance of various physio-chemical processes involved in the droplet combustion. This is accomplished by analysing the following major parameters which affect the combustion mechanism.

- (a) Size of the fuel droplets
- (b) Composition of the fuel
- (c) Composition of the gas (oxidant)
- (d) Relative velocity between the fuel droplets and gas
- (e) Ambient temperature
- (f) Ambient pressure

The results of this study would help to improve the knowledge of the combustion process through better understanding of the parameters which affect the combustion mechanism.

quantifier cette valeur qui ne peut être infinie. Or, personne d'autre que des hommes pourrait établir cette valeur. On revient donc à la position homocentrique de Jevons.

On peut considérer les langues comme des biens économiques de deux façons. D'abord on peut vouloir attribuer une valeur économique au code lui-même. Ainsi, il serait concevable qu'un groupe d'individus paie un spécialiste pour qu'il leur invente une nouvelle langue qui serait plus efficace que les langues traditionnelles. La somme que le spécialiste recevrait constituerait la valeur de cette langue que les acheteurs pourraient ensuite revendre sans jamais l'avoir parlée. C'est comme s'ils avaient acheté le brevet d'une invention d'un appareil quelconque. On peut acheter le brevet sans acheter l'appareil physique dont il constitue le principe.

La seconde façon de considérer les langues comme des biens économiques c'est de faire l'équivalence entre l'acquisition d'une langue et l'acquisition du mécanisme intellectuel qui permet l'utilisation du code. La possession d'une langue s'entend alors comme la possession d'un appareil mental permettant au cerveau de recevoir des informations qu'il ne pouvait auparavant recevoir directement. Acquérir une langue veut dire, dans ce sens, faire l'acquisition de cet appareil intellectuel qui permet d'interpréter les communications émises au moyen d'un code donné. En ce sens, il est commode de comparer l'acquisition d'une langue à l'acquisition d'un appareil comme un téléphone ou un téléviseur qui permet de bénéficier des communications

CHAPTER 2

COMBUSTION IN STAGNANT SURROUNDINGS

2.1 General

In considering combustion in stagnant surroundings, it is assumed that a single spherical burning drop is surrounded by a spherical symmetrical flame front as shown in Figure 1. In addition to a spherical symmetry, the following assumptions are usually made:

- (a) The droplet and flame form concentric spheres.
- (b) At an infinite distance from the drop lies a boundary at which the gas composition is that of the ambient gas.
- (c) Fuel vapour diffuses from the drop surface to the flame front and oxygen from the boundary in the ambient gas to the flame surface. The resulting combustion products diffuse from the flame to the surrounding gas.
- (d) Exothermic chemical reaction between the fuel vapour and oxidant takes place at the surface of stoichiometric composition.
- (e) Combustion occurs under iso-baric, quasi-steady state conditions.
- (f) Chemical reactions occur instantaneously and hence the reaction zone is infinitely thin.
- (g) Chemical reaction goes to completion and requires no activation energy.
- (h) Part of the heat of combustion is transmitted by conduction to the droplet to affect vaporization while the rest enters the ambient gas.

2.1 General (Cont'd)

- (i) The droplet temperature is uniform and equal to the boiling point of the liquid.
- (j) Radiation and thermal diffusion effects are negligible.

One of the primary assumptions of the above model is that all the fuel reaching the flame front is instantaneously consumed under steady state conditions.

It follows, therefore, that the combustion rate is controlled by the rate of vaporization of the liquid drop, which in turn, is determined by the rate of heat transfer to the drop.

2.2 Steady State

Godsave's [22] was one of the first theoretical attacks on the problem. Using some of the above mentioned assumptions and considering a steady state radial heat transfer from the flame to the drop against outward diffusing vapour, Godsave solved the resulting Fourier-Poisson equations to obtain the following expression for the mass burning rate:

$$\frac{dm}{dt} = \frac{2\pi k d \ln \left\{ 1 + c \left(\frac{T_f - T_s}{Q - R_a} \right) \right\}}{c \left(1 - \frac{d}{d_f} \right)} \quad (1)$$

2.2 Steady State (Cont'd)

k and c are the mean values of the thermal conductivity and specific heat in the region between the droplet surface and the flame front.

$$R_a = A_r / (dm/dt)$$

where A_r = the rate at which radiation is absorbed by the drop

$\frac{dm}{dt}$ = mass burning rate

d = drop diameter

d_f = flame diameter

T_f = flame temperature

T_s = surface temperature of the drop.

Q = latent heat of vaporization at the boiling point.

As no use was made of the assumption that oxygen diffuses to the flame, the position of the flame surface relative to the drop is not given by this theory. Experimental values of T_f have to be used to calculate $\frac{dm}{dt}$ from Equation 1.

T_f can be readily obtained from Spalding's Work [78] (see Figure 2).

Long [54] extended this theory by considering a heat balance between the flame and the droplet surface and an oxygen mass balance beyond the flame. His expression for the mass burning rate does not contain the term T_f and hence its solution does not require the use of empirical data.

2.2 Steady State (Cont'd)

$$\frac{1}{\pi d^2} \frac{dm}{dt} = \frac{2k}{cd} \left[\ln \left\{ 1 + c \frac{(T_f - T_s)}{Q} \right\} \right] + \frac{\rho D}{16 \chi d} \ln \frac{1 + N_{\infty}}{\chi} \quad (2)$$

where, ρ = mean density of oxygen beyond the flame

D = mean diffusivity of oxygen beyond the flame

χ = number of moles of combustion products derived from stoichiometric combustion of unit mass of fuel with oxygen

N_{∞} = mole fraction of oxygen in the bulk surrounding gas

χ = number of mole of oxygen required for stoichiometric combustion of unit mass of fuel

Goldsmith and Penner's theory [25,26] is basically a refinement of Godsave's. Use was made of all the above assumptions. Equations of conservation of energy and of continuity were applied to spherical shells of diameter d_1 and d_2 where $d_1 < d_f$ and $d_2 < d_{\infty}$. Integrating these, they obtained expressions for the mass burning rate. k and c are assumed to be linear functions of temperature.

$$k = k_1 \left(\frac{T}{T_s} \right) \quad (3)$$

$$c = a' + b'T \quad (4)$$

The mass burning rate,

$$\frac{dm}{dt} = \frac{2\pi k_1 d_1}{T_s b' (1 - \frac{d_1}{d_f})}$$

$$\ln \left\{ 1 + \frac{(T_f - T_s)}{Q} \left(a' + \frac{b'}{2} \right) (T_f + T_s) \right\} - \frac{a'}{\xi} \ln \left\{ \frac{(a' + b' \frac{T_f - \xi}{T_f + \xi})}{(a' + b' \frac{T_s + \xi}{T_f - \xi})} \right\} \quad (5)$$

$$\text{where } \xi = \sqrt{a'^2 - 2b' \left(Q - \frac{b'}{2} T_s^2 - a' T_s \right)} \quad (6)$$

k_1 = thermal conductivity of vapour inert gas mixture at temperature T_s .

d_1 = drop diameter

a', b' = constants

2.2 Steady State (Cont'd)

The theory further predicts that $df/d\ell$ should be constant for given values of the physico-chemical parameters.

The same basic equations have been used by others [32, 63, 93, 95] to obtain expressions for the mass burning rates. Usually assumptions have been made about the properties of the vapour-gas mixture between the droplet surface and the flame. For example, Wise et al. [93] assumed that ρD and $\frac{c}{k}$ were constants, while Hottel et al. [32] used a log mean value of $\frac{k}{c}$ in this region.

Some of these workers [69, 95] also derived expressions for the flame temperature T_f , the mass fraction of fuel vapour at the droplet surface, Y_f and the ratio of flame to drop radius $\frac{r_f}{r_d}$.

Further by this method, it is possible to deduce the temperature and composition profiles in the flame surrounding the drop. This has been achieved by Goldsmith and Penner [26] and by Wise et al. [95].

The expressions due to Wise et al are given below:

$$T_f = T_s + \frac{H - Q}{c} - \left\{ \frac{\left(\frac{H - Q}{c} \right) + T_s - T_g}{\left(1 + \frac{Y_{x\infty}}{i} \right)} \right\} \quad (7)$$

$$\frac{r_f}{r} = \ln \left\{ \frac{\frac{H}{Q} \frac{Y_{x\infty}}{i}}{\ln \left(1 + \frac{Y_{x\infty}}{i} \right)} \right\} \quad (8)$$

$$Y_F = 1 - \frac{Q}{H} \left(1 + \frac{i}{Y_X} \right) \quad (9)$$

where H = heat of combustion

2.2 Steady State (Cont'd)

T_g = temperature of ambient gas

i = Stoichiometric ratio

y_{∞} = mole fraction of oxidant infinity

y_F = weight of fraction of fuel vapour at the droplet surface

Spalding [78, 81] approached the problem in a slightly different manner. He postulated that combustion takes place in a stagnant film adhering to the droplet surface (see Figure 1). In this method, the fuel to oxidant ratio at the flame, and the following main transport processes occurring within the film are considered:

- (i) Diffusion of oxygen from the outer edge of the film to the flame surface.
- (ii) Conduction of heat from the flame to the droplet.
- (iii) Heat transfer from the flame to the ambient gas.

Solution of these equations gives:

$$\frac{dm}{dt} = 2\pi d \frac{k}{c} \ln(1 + B) \quad (10)$$

$$\text{where } B = \frac{H}{Q} \frac{M_{O_2}}{i} + c \frac{(T_g - T_s)}{Q} \quad (11)$$

(B has been termed transfer number)

Expression can also be obtained for T_f , d_f and $\frac{df}{d\ell}$ by this method.

Brzustowski [9] used Spalding's approach to consider the limitations imposed upon the validity of the physical model by chemical and evaporation kinetics and by high ambient pressures.

Simplification of the equations (1), (2), (5) and (10) leads to:

2.2 Steady State (Cont'd)

$$\frac{dm}{dt} = K_{10} d_{\ell} \quad (12)$$

since all other terms in these quotations can be assumed to be constants.

Where K_{10} = constant

d_{ℓ} = drop diameter.

Since mass burning rate, $\frac{dm}{dt}$ is defined as the time rate of change of mass of the droplet, equation 12 can be written as:

$$\frac{d}{dt} \left(\frac{\pi}{6} \rho_{\ell} d_{\ell}^3 \right) K_{10} d_{\ell} \quad (13)$$

Where ρ_{ℓ} density of the drop, which is assumed constant. Re-arrangement and integration of the equation 13 for the boundary conditions

$d_{\ell} = d_0$ at $t = 0$ leads to:

$$d_0^2 - d^2 = - \frac{4K_{10}t}{\pi \rho_{\ell}} \quad (14)$$

$$d_0^2 - d^2 = \lambda t \quad (15)$$

$$\text{where } \lambda = - \frac{4K_{10}}{\pi \rho_{\ell}} \quad (16)$$

From the equations (12), (14) and (16) it can be shown that λ is related to $\frac{dm}{dt}$ by the following equation:

$$\lambda = - 4 \frac{\frac{dm}{dt}}{\pi \rho_{\ell} d} \quad (17)$$

Table 1 shows the comparison of experimental and calculated values of burning constants.

2.3 Unsteady Effects

The simple quasi-steady constant property analysis of Godsave [22] is widely accepted theoretical model of liquid droplet combustion. The important analytical results of this theory which have been extended by other workers are presented in Table 2.

2.3 Unsteady Effects (Cont'd)

Table 2 compares the prediction of quasi-steady state with representative data obtained by different experimental techniques. It is clear that quasi-steady state predictions are not accurate, particularly with respect to the flame to drop diameter ratio and flame temperature. Such discrepancies between the prediction of quasi-steady and the experimental results have been attributed to various factors: finite kinetics, unsteadiness of the combustion process, variation of thermodynamic and transport properties and natural convection.

In view of the above, one of the explanations for these discrepancies lies in the non-steady or variable properties.

A number of workers have carried out the investigation, Some of the important work is given below.

The unsteady analysis of Isoda and Kumagai [38] considers only gasphase (g phase) unsteadiness while neglecting radial convection terms. The solution of the conduction equation involves the steady-state boundary conditions:

$$\frac{dT}{dr} = \dot{m} (H-L) / 4 \pi r_f^2 k \quad \text{at } r = r_f \quad (18)$$

$$\text{and } T = T_f$$

$$\text{and } T \rightarrow T_\infty \text{ as } r \rightarrow \infty \quad (19)$$

$$\frac{T - T_\infty}{T_f - T_\infty} = \frac{r_f}{r} \operatorname{erfc} \frac{r - r_f}{2 (\kappa_{gt})^{1/2}} \quad (20)$$

For the condition (experimental d^2 law) used by Isoda and Kumagai [38] Equation 20 with boundary condition (18) and (19) predicts steady quasi-state solution for d_f/d_s at large times (1.5 sec.). Another model of

2.3 Unsteady Effects (Cont'd)

g phase unsteadiness presented in the same report draws heavily from experimental results and does not constitute a proper check on the theory.

Kotake and Okazaki [44] replaced the quasi-steady state model with an unsteady state diffusion controlled model but retained most of the assumptions of the older theory.

The equations of mass concentration, temperature and velocity of the gas surrounding the droplet were written in finite difference form with respect to time and space. These were then solved numerically using stepwise increments of time. The results can be summarized as:

- (i) The $\frac{df}{d\lambda}$ predicted is in the same range as the experimentally observed one.
- (ii) The values of $\frac{d}{dt} (d^2)$ presented in Figure 3 show a larger initial slope and a smaller constant slope after a significantly long time. But the observed experimental trend (also shown in Figure 3) show just the opposite, namely a smaller initial gradient which quickly approaches a constant value.
- (iii) The theoretical life time of the droplets as seen from d_λ^2 against t graphs (Figure 3, Curves 1&2) is very much smaller than the time observed in experiments. For instance, for a 2 mm diameter benzene droplet burning in air at 300°C, the value is about 1.8 sec. A simple calculation i.e. use of the quasi-steady expression (Equation 10) to scale down the observed burning times at room temperature ($t_b = d_o^2/\lambda$) to that at 300°C. would show that t_b for 2 mm droplet should be about 4.5 sec. The plot of

2.3 Unsteady Effects (Cont'd)

Kobayasi [43] also shows that at as high an ambient temperature as 800°C, a smaller droplet of benzene ($d_0 = 1.4\text{mm}$) will take 1.8 sec. to burn out completely (Curve 3 in Figure 3). Finally, in reference [44] the plot of d_f/d_0 and T_f against time show a continuous increase till the end where the maximum T_f reached is much lower than the adiabatic flame temperature. It therefore follows that the numerical solution of Kataka and Okazaki [44] is suspect.

Further, a recent study on droplet evaporation by Hubbard et al [35] suggests that the numerical results of [44] are in error. Hubbard et al have also shown that gas phase unsteadiness is insignificant in evaporation process. The recent report of Waldman [88] on the non-steady combustion of a droplet is based on a symptotic analysis. His result, particularly on the variation of d_f/d_0 , with time, show discrepancies when compared with the experiment.

Ignition and Extinction of a Droplet

These phenomena are transient, hence the quasi-steady state theories can not explain them. A number of qualitative analysis have been made of these processes: [67, 68].

All these theories postulate that ignition is a process involving the transition from chemically controlled to diffusional controlled combustion. The theories predict:

- (i) The auto-ignition temperature of a droplet increases with decrease in droplet diameter.

2.3 Unsteady Effects (Cont'd)

Ignition and Extinction of a Droplet (Cont'd)

- (ii) The auto-ignition temperature is a weak function of ambient oxygen concentration for all but low oxygen concentration.
- (iii) The auto ignition temperature is strongly dependent on such chemicals' kinetics parameters as: the pre-exponential factor, overall reactor order, and some time activation energy.

Spalding [79] has proposed that the extraction of a droplet will occur when the mass rate of evaporation exceeds the minimum rate of consumption of the vapour in the flame. According to Spalding, the maximum rate combustion occurs with premixed stoichiometric flame. Spalding's view is supported by other workers [67].

Theoretical work carried out by Wise and Ablow [94] on the penetration of a thermal wave into a liquid droplet during ignition and combustion shows that a finite period of time must elapse before the centre of the droplet attains the surface temperature.

Wise and Ablow solving the equation of heat conduction numerically derived the temperature distribution within a droplet as a function of the group $(\frac{\lambda}{8\alpha})$, λ being the burning constant and α the thermal diffusivity of the liquid.

When $\frac{\lambda}{8\alpha}$ is 1, the centre of a droplet attains 90% of its surface temperature during the first half life of the droplet but 12% if $\frac{\lambda}{8\alpha}$ is 2. The assumption made by Wise and Ablow that T_s is constant throughout and that the burning rate is unaffected by gradual heating

2.3 Unsteady Effects (Cont'd)

Ignition and Extinction of a Droplet (Cont'd)

of the droplet implies that observable k , $\frac{d_f}{dx}$ and T_f are not affected by heating, a feature which is physically inappropriate. In order to arrive at an acceptable solution, it is necessary that variation of T_s and \dot{m} , with time, should be taken into account in any analysis on these basis, one can judiciously conclude that unsteadiness in droplet combustion occurs during a fraction of the total burning time in the initial stage. Unsteadiness being relevant only for obtaining time variation of d_f and d_f^2 and not for the steady values. It can further be said that the discrepancies between experimental observation and the prediction of constant property quasi-steady analysis cannot be attributed to unsteadiness.

2.4 Kinetic Effects

General

Several attempts have been made to examine quantitatively conditions under which chemical kinetics might affect the combustion rate and to test the accuracy of the assumption of an infinite chemical reaction rate.

Lorrel et al [55] considered a finite reaction rate of the bimolecular Arrhenius form: $\text{Rate} = A' (\text{fuel}) (\text{oxygen}) e^{-E/RT}$ and solved the conservation equations numerically for an ethanol droplet of diameter 0.04 cm burning in air and in oxygen. Values of E of 0.25, 0.50 kcal/mole were assumed. The results did not differ greatly from those calculated assuming an infinite chemical reaction rate. They have

2.4 Kinetic Effects

General (Cont'd)

concluded that kinetics can only seriously affect the combustion rate when either the droplet size is small or the ambient pressure is very low. Tarifa et al [85] using a similar approach, also came to this conclusion.

Williams [91] has used the Schawb-Zeldovich procedure to obtain the expression:

$$\frac{dm}{dt} = 2\pi d \frac{k}{c} \ln(1+B) - 2\pi dk H \frac{Y_{O_2}}{c Q} \quad (21)$$

$$\text{Where } B = \frac{H}{Q} M_{O_2} + c \frac{(T_g - T_s)}{Q} \quad (22)$$

which includes a correction term for finite chemical kinetics.

2.5 Oxygen/Fuel Ratio

Some of the seemingly realistic values of d_f/d_l have been obtained by the choice of low stoichiometric ratio by some investigators [42, 68]. A few experimental observations suggest that complete oxidation of the fuel may not take place at the flame zone.

The soot formation during combustion of droplets [43] and the presence of significant amount of carbon monoxide even beyond diffusion flame zone [64] are definite indications of oxygen/fuel being lower than stoichiometric at the flame zone.

The variation of oxygen/fuel may be used only to obtain an indication of the kinetic effect, as the use of lower oxygen/fuel than stoichiometric value is contradictory to the theory using a single-step reaction with thin flame kinetics.

CHAPTER 3

EFFECT OF VARIABLE PROPERTIES IN COMBUSTION

CHAPTER 3

EFFECT OF THE VARIABLE PROPERTIES IN COMBUSTION

3.1 Review of the Existing Work

The thermodynamic and transport properties involved in the theoretical analysis of droplet combustion are specific heat at constant pressure (C_p), thermal conductivity (k) and diffusion co-efficient. In actuality, these vary with both concentrations and temperature and since the combustion of a droplet involves strong variations of these quantities, such variations may be expected to affect the overall results significantly.

Goldsmith and Penner [26] introduced the variation of fuel specific heat and thermal conductivity as linear function of temperature into the simple theory of Godsave [22] and extended it to obtain the relation for flame position and temperature. However, the calculated values of burning constant are much too high. This is evidenced by the fact that they correspond to values derived from experiment with natural convection [48] which enhances the burning rate. Similarly, the estimated flame temperatures are also very high even when compared with constant property predictions. The linear variation of specific heat with temperature ($C_p = a_1 + b_1 T$) employed by them [26] is compared with the values from Svehla's tables [84] in Figure 4. It is evident that the relation is unrealistic, particularly when the flame temperature obtained is as high as 3400°K. In addition, the result for d_f/d_d seem to be extremely sensitive to variation in b_1 ,

3.1 Review of the Existing Work (Cont'd)

particularly in the range $0 < b < 10^{-4}$ (see Figure 5). A small gradient in Cp-T relation produces surprisingly large change in $df/d\lambda$.

Williams [93] has obtained a set of relations for combustion parameters hereby arbitrary dependance of D and Cp on temperature are allowed.

(Lewis number is taken as unity.) The merit of this work in comparison with experimental results are not easily seen, as no numerical results are presented.

Kassoy and Williams [42] have introduced k and D variation (with temperature only) in their analysis using singular perturbation technique but have considered Cp as a constant. They have used a value of unity for the stoichiometric rates (which is seldom true for a liquid hydrocarbon-oxygen system) and therefore, the predicted low $df/d\lambda$ (~ 10) is not surprising. At such Q/F even quasi-steady-state theory predicts low values of $df/d\lambda$ (Eq. 10). It may be noted that in their modified flame surface theory, Pesin and Wise [68] have also used a value of unity for Q/F and consequently, have arrived at low $df/d\lambda$ (~ 10).

So far, no investigators have incorporated the detailed variation of Cp and k (with temperature and concentration). The effect of the Lewis number ($\rho dCp/k$) and variation of Q/F at flame as well, the application of temperature dependent thermodynamic properties in the quasi-steady state theory, would considerably change the behaviour of combustion.

3.1 Review of the Existing Work (Cont'd)

In view of the above, the introduction of the temperature dependent thermodynamic properties in the quasi-steady state theory would considerably alter the behaviour of combustion and is likely to give more realistic prediction of the burning. Further, the Lewis number ($\rho_d C_p / k$) and variation of O/F at flame would significantly effect the combustion.

3.2 Calculation of the Parameters Affecting the Combustion of the Droplet

3.2.1 Method of Evaluating Thermodynamic and Transport Properties of the Fluid

(a) Prediction of Thermal Conductivity

Thermal conductivity of the droplet fuel at various temperature can be calculated by using the following empirical relationship:

$$K_p = A + BT + A \left\{ (20/3) [1 - D(1 - T)^c] (1 - T_r)^{2/3} \right\} \quad -50^\circ R < T < 1500^\circ R$$

where K_p = thermal conductivity BTU/ft hr F.

T = temperature, $^\circ R$

T_r = reduced temperature, T/T_c .

Constant A, B, C and D in the above equation have been experimentally evaluated and given below for single component fluid:

FLUID	CONSTANTS			
	A	B	C	D
Benzene	0.01697	0	1.0	0
Toluene	0.01505	0	1.0	0
Acetone	0.037	0	-0.3	0.46

3.2.1 Method of Evaluating Thermodynamic and Transport Properties of the Fluid (Cont'd)

(a) Prediction of Thermal Conductivity (Cont'd)

Using the above relationship, the computer program has been developed, and thermal conductivity of Benzene has been calculated at various temperatures (see Appendix B).

(b) Prediction of Specific Heat

Attempts have been made to predict specific heat using thermodynamic equations, but this has not yielded results which could be correlated with the experimental values.

In view of this curve fitting experimental c_p data for gases, using an exponential model:

$$c_p = A + Be^{-c/T^n}$$

where c_p = ideal-gas specific heat. A, B, C, and n are constant in the above equation; have been used and which have been shown to be superior to the commonly used empirical forms. The data for constants used is based on the experimental values commonly available in the range of 460°R-2000°R.

The constants used in the above equation are given below.

FLUID	CONSTANTS			
	A	B	C	n
Benzene	8.5813	65.2801	1167.483	1.1377
Toluene	13.1234	79.9036	1228.2582	1.1337

3.2.1 Method of Evaluating Thermodynamic and Transport Properties of the Fluid (Cont'd)

(b) Prediction of Specific Heat (Cont'd)

Based on the above data, the values of heat capacity at various temperatures for Benzene have been computed using digital computer. Calculated values of the specific heat at various temperatures are given in the computer print-out Appendix B.

Computer print-out appended in Appendix B also presents all thermodynamic and transport properties for Benzene which have been utilized in the analysis contained in this dissertation.

3.2.2 Method of Evaluating the Parameters Affecting the Combustion of the Droplets

Most of the investigators have predicted the behaviour of the combustion using constant thermodynamic and transfer properties. In this study, in the first instance, the burning constant λ is obtained at constant c_p , and all other parameters are evaluated using variable properties. The result is presented in Table 3.

In the second instance, the burning constant λ , is calculated at variable thermodynamic properties using Equation 17. The value of the variable k and the other variable thermodynamic and transfer properties are used to calculate the value of $\frac{df}{d\eta}$ and T_f and these are presented in Table 4.

3.2.2 Method of Evaluating the Parameters Affecting the Combustion of the Droplets (Cont'd)

In the constant property approximation [Table 3] the constant value of $\lambda(1.12)$ is chosen such that the prediction of λ is realistic [Table 2] and occurs at point where temperature is 400°C . This is much below the arithmetic mean of surface and flame temperature. Also, the location of this temperature is close to the surface as expected. Table 4 also demonstrates that the improvement in the prediction of $\frac{df}{dt}$ is significant when variable c_p and k are employed. The prediction of λ ($0.98 \text{ mm}^2/\text{sec}$) agrees with the experimental observations fairly well and the predicted flame temperature is in the same region as the adiabatic temperature. However, values of $\frac{df}{dt}$ and T_f are still larger than the experimentally observed value. Further improvement of the theoretical predictions can be achieved by the inclusion of the radiation effect.

CHAPTER 4

COMBUSTION IN CONVECTIVE GAS FLOW

CHAPTER 4

COMBUSTION IN CONVECTIVE GAS FLOW

4.1 General

A spherical symmetrical fuel droplet burning is only mathematically tractable in a stagnant atmosphere.

If the stagnant film of thickness δ is assumed to exist, then free stream conditions are thought to exist at some distance χ from the fuel surface. Within the stagnant film, the mass transfer rate could be evaluated by solving the energy equation incorporating the necessary boundary conditions. However, when the free stream, whether forced or due to buoyancy effect is transverse due to the mass evolution from the regressing fuel, a stagnant film does not exist and therefore the solution to obtain would not be explicitly correct.

The presence of natural convection in droplet combustion destroys the spherical-symmetry of combustion and distorts the flame from its spherical shape (see Figure 6).

In such cases, the calculation of the mass burning rate of a droplet experiencing convection would require solution of the equations of conservation of energy, of continuity and of the Navier Stokes equations. The boundary conditions for solving latter would be complex and non-linearly would arise because of the inertia term of Navier-Stokes equation. Under this condition, an analytical solution is not possible.

4.2 With Natural Convection Effects

As a result, the effect of natural convection on the burning rate has been taken into account by means of empirical correlations. Two of these are noted below:

- (i) Spalding's Relation [78]

$$\dot{M}_n = 0.45 \frac{k}{c} B \frac{1}{d} \left(\frac{g d^3}{2} \right)^{\frac{1}{4}} \quad (23)$$

which is valid for $0.25 < B < 3$

- (ii) Agoston et al Relation [2]

$$\dot{M}_n = \dot{M}_s \left(1 + \frac{0.20}{B} \text{Gr}^{0.3} \right) \quad (24)$$

Log mean temperature should be used in calculating the physical properties and Gr.

The above empirical relations have yielded good agreement under natural convection and unsteady conditions.

4.3 With Forced Convection Effects

The forced convection can affect the combustion of droplet in a number of ways [29] :

- (a) There is a considerable deviation of the flame from spherical symmetry.
- (b) The film thickness is not infinitely large.
- (c) The total heat transfer and evaporation rates change over the drop surface.
- (d) The mass burning rate is higher than that predicted by the spherical symmetrical model.

The variation of the heat transfer rate over a droplet experiencing forced convection is shown in Figure 7.

4.3 With Forced Convection Effects (Cont'd)

For the sake of simplicity, however, most of the correlations of the burning rates neglect these changes and use an average value for the whole droplet. Some of the empirical and semi-empirical correlations of the mass burning rates of the droplets under forced convection conditions are presented in Table 6.

The increase in the burning rate with convection shown in Table 5 is because of the reduction in the thickness of the stagnant film beyond the flame front. This increases the oxygen concentration at the flame surface and so decreases the distance between the flame and the drop surface. Further, the burning constants are increased by the increase in relative velocity between a droplet and the ambient gas.

Empirical correlations have also been obtained between mass burning rate and Re (see Table 6).

Lumagai and Isoda [46] have obtained the following correlation for single droplets burning in vibrating air field.

$$\lambda_z = \lambda_s + K_1 f p_1^2 (K_2 - f p_1^2) \quad (25)$$

where λ_s = burning constant of the drop in stagnant medium

λ_z = burning constant with vibrations

K_1, K_2 = experimental constants

f = frequency of vibration

p_1^2 = amplitude of air vibration

4.3 With Forced Convection Effects (Cont'd)

The burning constant η_2 can be increased by up to 15% over the still air value, apparently by an increase in the gas diffusivity. Further increase in the vibration amplitude reduces the burning rate. This is attributed to the deformation of the flame boundary.

Forced convection can radically alter the type of the flame supported by a droplet.

Spalding [80, 81] observed envelope flames at low stream velocities. At speeds in excess of the extinction velocity, he reported that a flame could be stabilized behind the drop, which, he termed a wake flame. An envelope flame is a diffusion flame while a wake flame is of a premixed type.

A third type, namely a flame which is stabilized within the boundary layer at the side of a drop, has also been observed.

Eisenklam and Arunachalam [18] have found that the drag coefficients of burning drops are strongly influenced by the type of the flame associated with the drops. They found that the values of C_p for drops with side flames were less than the standard values, whereas those of the drops supporting envelope flames were higher. These values were calculated on the basis of approach properties, i.e. the properties of the undisturbed atmosphere in the chamber.

A number of measurements of the flame and internal drop temperatures have been made.

4.3 With Forced Convection Effects (Cont'd)

Experimental work on droplet temperatures [36, 37] suggests that the centre of the droplet is below the boiling point of the fuel until more than half the mass of the drop has been burnt.

Measured flame temperature [90] agree more with the calculated rich limit temperatures than with those calculated for stoichiometric combustion conditions.

In order to determine the penetration of a spray droplet experiencing forced convection in a gas flow within a reactor, a knowledge of drag coefficient of both burning and unignited drop is required. The behaviour of inert spheres while under-going momentum transfer forms a useful starting point.

Calculation of the drag coefficient of a sphere requires the solution of the Navier-Stokes' equations for the flow around the sphere. However, complete analytical solution of the Navier-Stokes equation has not been obtained for $Re \gg 1$ due to its nonlinear inertia terms. However, various experimental data on C_d obtained from smooth non-rotating solid spheres moving with constant velocities in infinite media can be related by a single curve with C_d and Re as co-ordinates. This is frequently referred to as the standard curve. A typical curve is shown in Figure 8. A number of analytical methods used in calculating the drag coefficients for the combustion of a droplet in a forced convective atmosphere are given in Appendix A.

CHAPTER 5

HEAT TRANSFER BY RADIATION TO A FUEL DROPLET

CHAPTER 5

HEAT TRANSFER BY RADIATION TO A FUEL DROPLET

5.1 General

In spite of the voluminous amount of literature on single droplet combustion, most studies on drop flames have ignored radiative energy transfer to the drop, mainly because of the lack of experimental data. It is, however, felt that drop flame emits appreciable radiation under conditions causing the formation of soot.

Even though certain aspects of the combustion of the single droplet under radiative heat transfer is understood, the mechanism of the combustion of a single droplet under radiative heat transfer is not quantitatively understood. There is, at present, difficulty in the rigorous approach to the analysis from first principal of this problem.

In this section, attempts have been made to develop a semi-analytical technique to evaluate the radiative heat transfer resulting from the combustion of a single droplet.

The rate of radiative heat transfer from the flame to the drop is given:[96]

$$R_a = \alpha_d \epsilon_f SA \sigma (T_f^4 - T_s^4) \quad (26)$$

where R_a = heat transfer by radiation

A = surface area of the drop

α_d = absorptivity of the drop

ϵ_f = emissivity of the flame

σ = Stefan - Boltzmann's constant

T_f = flame temperature

5.1 General (Cont'd)

T_s = surface temperature of the drop

S = solid angle of effective radiation

Based on the experimental work of Wolfhard and Parken [96] that hydrocarbon droplets are more or less transparent to all wave lengths upto 6.4μ with the exception of C H band at 3.54μ and 93% of the radiation lies within this region, the effective radiation constants of the equation (26) would be developed analytically.

5.2 Emissivity

Radiation from residual droplet is due, in part, to burning coke particles formed by asphaltiness in the oil. When the perimeter of a particle is less than six-tenths the wavelength measured in the particle, the particle acts like a point-source of volume - Rayleigh particles.

It is commonly assumed that the luminosity in diffusion flame is caused by the soot, though some doubt exists [15]. Soot particles in diffusion flame are generally small so that the spectral absorption co-efficient ρ_s can be calculated from small particle limit of Mie theory [33] making it proportional to the volume fraction of the particles.

The monochromatic absorption is then independent of the particle size and proportional to the volume function $f_v = \rho_c c_m$ where c_m is mass concentration and ρ is particle density and to the reciprocal of Wave length $\frac{1}{\lambda}$. The proportionality constant K depends on the refractive index n and absorption index k . The emissivity is then given by:

$$\epsilon_{\lambda} = 1 - e^{-[K(n, k)]^f \frac{L}{\lambda}} \quad (27)$$

5.2 Emissivity (Cont'd)

On the assumption that n and k are independent of wave length and temperature, k (n, k) in the equation (27) becomes constant, the total emissivity may be calculated with spectral distribution of blackbody radiation expressed by Wien's equation rather than Planck's because of the low λT range of main interest.

$$\begin{aligned} \epsilon_g &= \frac{\int_0^\infty \epsilon_\lambda E_\lambda d\lambda}{\int_0^\infty E_\lambda d\lambda} \\ &\approx \frac{\int_0^\infty (1 - e^{-\frac{h f_v \lambda}{k T}}) c_1 \lambda^{-5} e^{-c_2/\lambda T} d\lambda}{\int_0^\infty c_1 \lambda^{-5} e^{-c_2/\lambda T} d\lambda} \end{aligned} \quad (28)$$

Rearranging the above equation by defining $X = c_2/\lambda T$

and $Y = \frac{1}{\lambda T} (c_2 + h f_v \lambda T)$

$$\epsilon_g = 1 - \frac{\frac{c_1 T^4}{(c_2 + h f_v \lambda T)^4} \int_0^\infty y^3 e^{-y} dy}{\frac{c_1 T^4}{c^4} \int_0^\infty x^3 e^{-x} dx} \quad (28a)$$

5.2 Emissivity (Cont'd)

The definite integral are gamma function $\Gamma(4)$, cancels out and total emissivity reduces to:

$$\xi_g = 1 - \left[\frac{1}{1 + Kf_v \cdot LT/C_2} \right]^4 \quad (29)$$

Some experimental work at Ijmuiden on two types of oil flame yields values of 4.4 and 9.8 for k/c_2 ; a tentative value of $5 \text{ cm}^{-1} \text{ } ^\circ\text{K}^{-1}$ ($85 \text{ ft}^{-1} \text{ } ^\circ\text{R}^{-1}$) could be taken.

Elsasser model can be used to predict the proportionality of $1/T$ to L [17].

5.3 Absorption

The effect of internal absorption is of great interest in radiative transfer to the combustion of a droplet. This can be determined by using the analogy of a beam incident on a sphere at an angle θ . Considering the grey-plus-clear model and using the Fresnel's equations [33].

In spectral regions of Isotropic Dielectric Media ($k=0$), where the absorption index is negligible, the radiative properties of dielectrics are determined entirely by the refractive index n which is equal to $\sqrt{\epsilon}$. Radiation incident on a surface at an angle θ' to the normal will undergo partial specular reflection and partial refraction, the angle of refraction is given by Snell's law.

$$\sin \theta' = n \sin \theta/n \quad (30)$$

5.3 . Absorption (Cont'd)

The reflectivities of the components of polarization resolved parallel and perpendicular to the plane of incidence are best considered separately. They are:

$$\rho_{\perp} = \frac{\sin^2 (\theta - \chi)}{\sin^2 (\theta + \chi)} \quad (31)$$

and

$$\rho_{\parallel} = \frac{\tan^2 (\theta - \chi)}{\tan^2 (\theta + \chi)} \quad (32)$$

Elimination of χ among (30), (31) and (32) gives:

$$\rho_{\perp} = \frac{(n^2 - \sin^2 \theta)^{\frac{1}{2}} - \cos \theta}{(n^2 - \sin^2 \theta)^{\frac{1}{2}} + \cos \theta}$$

and

$$\rho_{\parallel} = n^2 \cos \theta - (n^2 - \sin^2 \theta)$$

These are known as Fresnel's equation.

For normal incidence ($\theta = 0$)

$$\rho_{\perp} = \rho_{\parallel} = (n^2 - 1) / (n^2 + 1)^2$$

and at glancing incidence ($\theta = \pi/2$)

$$\rho_{\perp} = \rho_{\parallel} = 1$$

Integrating over all angle of incidence would yield the desired values of absorption constant for Gray-Body and Gray-plus-clear Model.

Calculated values of total absorption co-efficients are presented in Table 7.

5.3 Absorption (Cont'd)

Figure 9 shows the relationship of the total absorption and with KR for material of Refractive Index 1.5.

Figure 10 present the Directional Emmissivity of strong absorber.

Figure 11 shows the internal local volumetric absorption rate in an absorbing reflecting sphere, the surface of which is uniformly irradiated with hemispherical flux, Refractive Index 1.5.

CHAPTER 6

HEAT AND MASS TRANSFER FROM DROPS —

CHAPTER 6

HEAT AND MASS TRANSFER FROM DROPS

Heat and mass transfer from burning and evaporating droplets have been correlated by use of dimensionless groups. Some of the better known are:

Ranz and Marshall correlation [72]

$$\bar{Nu} = 2 + 0.6 Re^{\frac{1}{2}} Pr^{\frac{1}{3}}$$

Eisenklam et al relations [19]

$$\bar{Nu} = \frac{2 + 1.6 Re^{\frac{1}{2}}}{1+B}$$

for evaporation

$$\bar{Nu} = \frac{4.9 Re^{0.4}}{1+B}$$

for combustion

B and Re are calculated using mean values of the physical parameters.

CHAPTER 7

DISCUSSION

CHAPTER 7

DISCUSSION

7.1 General

The concept of burning of condensed phases is applicable to the droplet burning, the flame produced is diffusion flame. The condensed phase is considered as a liquid fuel and the gaseous oxidizer as oxygen; the fuel is evaporated from the liquid interface and diffuses to the flame front as the oxygen moves from the surrounding to the burning front.

The rate at which the droplet evaporates and burns is generally considered to be determined by the rate of heat transfer from the flame front to the fuel surface. The chemical processes are assumed to occur so rapidly that the burning rates are determined solely by mass and heat transfer rates.

Most of the analytical works consider a double-film for the combustion of the liquid fuel. One film separates the droplet surface from the flame front and the other separates the flame front from the surrounding oxidizer as depicted in Figure 12.

Survey of the temperature in burning liquid indicates that the temperature is only a few degrees below the boiling temperature. In all the approaches, all the droplets have been assumed to be at a uniform temperature and at the normal boiling point. In the vicinity of the flame surface, the fuel evaporates at the drop surface and diffuses towards the flame front where it is consumed. Heat is conducted from the flame front to the liquid and it vaporizes the fuel.

7.1 General (Cont'd)

Most analysis assume that fuel is heated to the flame temperature before it chemically reacts and that the fuel does not react until it reaches the flame front. This latter assumption means that the flame front is mathematically thin surface where the fuel and oxidizer meet in stoichiometric proportions.

In stagnant atmosphere the film boundary is assumed to be at an infinite distance from the fuel surface. However, in convective flow definite boundary layer exists, oxygen diffuses to the flame front and combustion product and heat are transported to the surrounding atmosphere. The position of the boundary is determined by convection. All the analysis have been carried out on the assumption that there is no radiant energy transfer.

The parameters which define the combustion parameters are:

- (a) the mass burning rate or burning constant (λ);
- (b) the flame position above the fuel surface or the ratio of the $\frac{\text{diameter of flame}}{\text{diameter of the drop}}$ $\left(\frac{d_f}{d_d}\right)$; and
- (c) flame temperature.

7.2 The Mass Burning Rate

The burning constant determines the burning rate. Values of B for various fuel are given in Table 8 (Spalding 1955). Examination of this table reveals that, variation in B for different fuel are not great. Indeed, for most industrial fuels, it varies only from 5.1 to 1.7. Since the transfer number always enters the burning rate

7.2 The Mass Burning Rate (Cont'd)

expression as a $\ln(1+B)$ term, one may conclude that as long as the diffusion atmosphere is kept the same, there will not be a great variation in the burning rate of various fuel. A tenfold variation in B results only in an approximately two fold variation in burning rate. A ten fold variation in the diffusivity or gas density would result in a ten fold increase in burning rate.

Further, the burning rate can be determined without determining the flame temperature or the position of the flame. It was necessary to find the flame temperature in all the theoretical works which followed the Godsave [29] approach. Most of the investigators made comparisons, not only of the calculated and experimental burning rate, but also of the flame temperature and position. Most of the experimenters found good agreement with respect to burning rate but poorer agreement in flame temperature and position. They had failed to realise that the burning rate is independent of the flame temperature.

Table 1 presents some typical values of the burning constant calculated from Equation 10 and B values in Table 8. The experimental measurements of various workers are also shown in Table 1. The agreement is good. These results show that the burning constant of fuels does not seem to be systematically influenced by the wide variation in their chemical structure. The general order of magnitude of λ for hydrocarbons burning in air is about 10^{-2} cm²/sec.

7.2 The Mass Burning Rate (Cont'd)

Of all the measurable quantities, the prediction of burning rate has been most successful in obtaining support by investigators (See Figure 13 and Tables 2,3,4), Quasi-steady state analysis predicts that the mass burning rate is proportional to the first power of the droplet diameter. This implies that the square of the diameter decreases linearly with time. The outstanding contribution of quasi-steady state theory has been in isolating the final functional dependence of \dot{m} on r_f equivalent, the d^2 law which has been observed in the experiments, but the quantitative evaluation of $\frac{\dot{m}}{r_f}$ or λ involves a judicious choice of the thermodynamics and transport properties. By comparison of quasi-steady state predictions with experimental results obtained under zero g [50], one can conclude that the prediction of \dot{m} is an overestimation. In fact, if the value of λ is evaluated at the mean temperature between the droplet surface and the flame, the estimated burning rate will be significantly larger than that which is actually observed. [3]

Further, the observed experimental result (Figures 3, 14) shows a smaller gradient which quickly approaches a constant value. The life time of droplet as seen from their d^2 against T graphs for a 2mm diameter benzene droplet burning in air at 300°C is about 1.8 sec. A simple calculation using quasi-steady expression (Equation 15) to scale down the observed burning time at room temperature, ($t_b = d_0^2/\lambda$) to that at 300° would show that t_b for the 2mm droplet should be about 4.5 sec; which goes to prove that life time of droplet predicted by quasi-steady theory is much higher than actual value.

7.2 The Mass Burning Rate (Cont'd)

The initial phase of burning where the relationship of the Equation (15), does not hold true has been identified as "the heating period".

7.3 The Ratio of Flame Diameter Drop Diameter (d_f/d_d)

Quasi-steady state theory predicts that $\frac{d_f}{d_d}$ is constant during combustion. The value of $\frac{d_f}{d_d}$ based on quasi-steady is an example of over-estimation (see Table 2). Because of its logarithmic dependence on B, $\frac{d_f}{d_d}$ has a negligible dependence on the chosen mean thermodynamic and transport properties (Equation 10). $\frac{d_f}{d_d}$ is considered to be independent of the diameter of the droplet in spite of the fact that experimental observation has recorded that the initial movement of the flame is away from the droplet followed by gradual decrease in size as the droplet continues to shrink steadily.

The discrepancy between the experimental values and the value of $\frac{d_f}{d_d}$ predicted by quasi-steady state theory has been attributed by a number of workers due to omission of convection.

7.4 Flame Temperature

Quasi-steady state theories predict that the flame temperature is constant and equal to the adiabatic flame temperature. The flame is formed at the locus where the ratio of fuel to oxidant flow is stoichiometric. Referring to Table 1, the theoretically predicted values of T_f have again been considerably larger than the experimental values.

7.4 Flame Temperature (Cont'd)

The free convection to all probability does not alter the flame temperature. In consequence, the inclusion of kinetics and unsteadiness becomes a necessary prerequisite for the realistic prediction of T_s . On this basis, T_s , $\frac{df}{dt}$, and T_f change during combustion, and therefore, a finite period of time must elapse before the centre of the droplet attains the surface temperature of the droplet. Radiation transfer from the gasses alter temperature both in the flame and in the droplet itself.

The radiation interaction lowers the predicted (quasi-steady state) temperature in high temperature region of the boundary layer near the flame front and raises the temperature in cooler region near the edge of the boundary. This affect would be greater in the presence of larger convective forces. The effect of radiation can be interpreted to result from a transfer of energy by gaseous radiation heat transfer from the hotter region to cooler portion, thus reducing the higher temperature and raising the lower one. This would tend to increase the thermal boundary layer thickness and this effect would be considerably increased with larger convection.

CHAPTER 8
CONCLUSION

CHAPTER 8

CONCLUSIONS

(a) The existing theories, if applied judiciously, can predict the behaviour of the combustion of a single droplet.

(b) Quasi-steady state theory predicts realistically d^2 law over a wide range, except over the initial 20-25% of the total life of the droplet, where the unsteady state prevails.

The burning constant can be predicted accurately by the use of quasi-steady state theory provided judicious use of the variation of the thermal conductivity and specific heat with temperature is taken into account in the calculation.

(c) The flame temperature can be realistically predicted by including the effect of radiation based on the actual condition of the flame viz. incomplete combustion or by taking this into account by equivalent low oxygen fuel ratio.

(d) The realistic prediction of the $\frac{d_f}{dt}$ demand that the analysis must take into account the effect of the convection, the decrease in the flame temperature resulting from the radiation and introduction of the realistic value of the transfer properties (viz. Lewis numbers for the flame and the drop) and temperature dependent thermodynamic properties.

TABLES

TABLE 1

BURNING CONSTANTS FOR VARIOUS HYDROCARBONS

(oxidant at 20°C and 1 atmosphere)

FUEL	BURNING CONSTANT λ mm ² /Sec.		EXPERIMENTOR
	CALCULATED	MEAN EXPERIMENTAL	
Benzene	1.12	0.97	Godsave
Benzene	1.12	0.99	Goldsmith
Toluene	1.11	0.66	Godsave
Toluene	1.11	0.77	Goldsmith
O-Xylene	1.04	0.79	Godsave
P-Xylene	1.08	0.77	Godsave
Ethyl Benzene	1.08	0.86	Godsave
Iso-propylbenzene	1.06	0.78	Godsave
Tertiary-Butylbenzene	1.04	0.77	Godsave
Pseudocumene	1.02	0.87	Godsave
Ethyl Alcohol	0.93	0.81	Godsave
Ethyl Alcohol	0.93	0.86	Goldsmith
Ethyl Alcohol	0.93	0.85	Wise
N-Heptane	1.42	0.97	Godsave
N-Heptane	1.42	0.84	Goldsmith
Iso-octane	1.44	0.95	Godsave
Iso-octane	1.44	1.14	Graves
DeCane	1.16	1.01	Hall
Kerosine ($P=0.805$)	0.97	0.96	Godsave
Diesel oil ($P=0.850$)	0.85	0.79	Godsave

TABLE 2

A GENERAL COMPARISON OF EXPERIMENTAL
DATA WITH QUASISTEADY STATE PREDICTION
(material: n-heptane)

TECHNIQUE	CONDITION	d_o (mm)	$\lambda = \frac{4m}{\pi r_o^2} \frac{d_o}{dt}$ mm/Sec	$\frac{df}{dq}$	T_f °K
Stationary suspended drop [3]	Unsteady, natural convection	1.5	1.1	3.0	1800
Porous burner [3]	Steady, natural convection	12.0 1.5*	1.8 1.04*	1.35 1.8	2000
Droplet in Zero "g" State [50]	Unsteady, no convection	0.95	0.78	6-10	
Quasi - Steady State Theory	Quasi-Steady, no convection	Any size	1.41	29.0	2300

*: Extrapolated value.

TABLE 3

COMPARISON OF COMBUSTION PARAMETERS
FOR BENZENE DROPLET OF 2mm IN ANALYSIS WITH CONSTANT k
AND VARIABLE THERMODYNAMIC PROPERTIES

COMBUSTION PARAMETERS	EXPERIMENTAL VALUE	CALCULATED VALUE	
		Cp, k Constant	Cp Constant and k variable
λ_{mm}^2/sec	0.97	1.12	0.735
d_f/d_e	6-10*	33.94	25.14
$T_f (^{\circ}K)$	2237	2748	2563

*: This value refer to an unsteady, no convection condition.
 Data for steady, no convection condition is not available.

TABLE 4

COMPARISON OF COMBUSTION PARAMETERS FOR BENZENE DROPLET
OF 2mm IN ANALYSIS WITH VARIABLE K AND
THERMODYNAMIC PROPERTIES

COMBUSTION PARAMETERS	EXPERIMENTAL VALUE	CALCULATED VALUE	
		Cp, k CONSTANT	Cp, k VARIABLE
λ_{mm}^2/sec	0.97	1.12	0.981
d_f/d_s	6-10*	33.94	18.47
$T_f (^{\circ}K)$	2237	2748	2563

*: This value refers to an unsteady, no convection, condition data for steady, no convection condition is not available.

TABLE 5

THE EFFECT OF AMBIENT GAS VELOCITY ON THE BURNING CONSTANT

Experimental Technique	Relative gas velocity	Change in the burning constant	Extinction velocity
Suspended drop technique Goldsmith [27]	Ambient gas velocity was raised from 0 to 40 cm/sec	36% increase in λ	Flame extinction occurred at a velocity greater than 40 cm/sec
Suspended drop technique Kumagai [49]	Ambient gas velocity was increased to 45 cm/sec	38% increase in λ	Flame extinction occurred at higher velocity (45 cm/sec)
Suspended drop technique (Furnace temperature = 700°C) Masdin [56]	Ambient gas velocity was increased from 0 to 15 cm/sec	10% increase in λ	Auto ignition failed to occur at higher velocity

TABLE 6

VARIOUS CORRELATIONS OF THE MASS BURNING RATE OR MASS RATE
EVAPORATION UNDER FORCED CONVECTION CONDITIONS.

Name of investigators	Experimental	Empirical or semi-empirical correlations	Comments
Frossling [20]	At room temperature Nitrobenzene, Naphthaline, where $2 < Re < 800$	$\dot{M}_f = \dot{M}_s (1 + 0.276 Re^{1/2} Sc^{1/3})$	
Ranz & Marshall [71]	Up to 200°C ambient temperature	$\dot{M}_f = \dot{M}_s (1 + 0.3 Re^{1/2} Sc^{1/3})$ for high temperature evaporation or drop-let combustion it is customary to replace Sc by Pr so that \dot{M}_f is given by $\dot{M}_f = \dot{M}_s (1 + 0.3 Re^{1/2} Pr^{1/3})$	
Agoston et al [2]	At 2,200°K - 2,920°K Ethanol and Methanol burning from a model sphere	$\dot{M}_f = \dot{M}_s (1 + 0.24 Re^{1/2})$	Pr was assumed constant and equal to 1
Spalding [78]	Model sphere technique $800 < Re < 4000$, $0.6 < B < 5$	$\dot{M}_f = 0.53 B^{3/5} Re^{1/2} / d$	B is transfer number and is defined by equation 11
Eisenklam [19] et al	Freely moving burning drops $0.1 Re < 5$	$Nu = \frac{4.9}{1+B} Re^{0.4}$	

TABLE 6 (cont'd)

VARIOUS CORRELATIONS OF THE MASS BURNING RATE OR MASS RATE
OF EVAPORATION UNDER FORCED CONVECTION CONDITIONS

Name of investigators	Experimental conditions	Empirical or semi-empirical correlations	Comments
How (34)	For burning or evaporating drops	$\dot{M}_f = \dot{M}_s \times (1 + 0.22 Re^{\frac{1}{2}})$	

TABLE 7

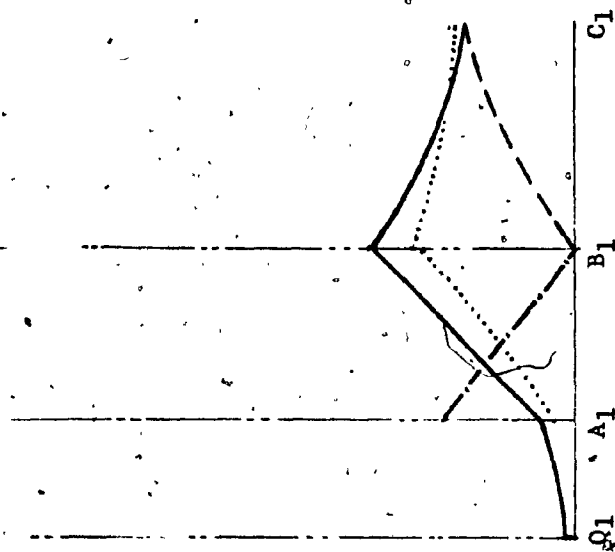
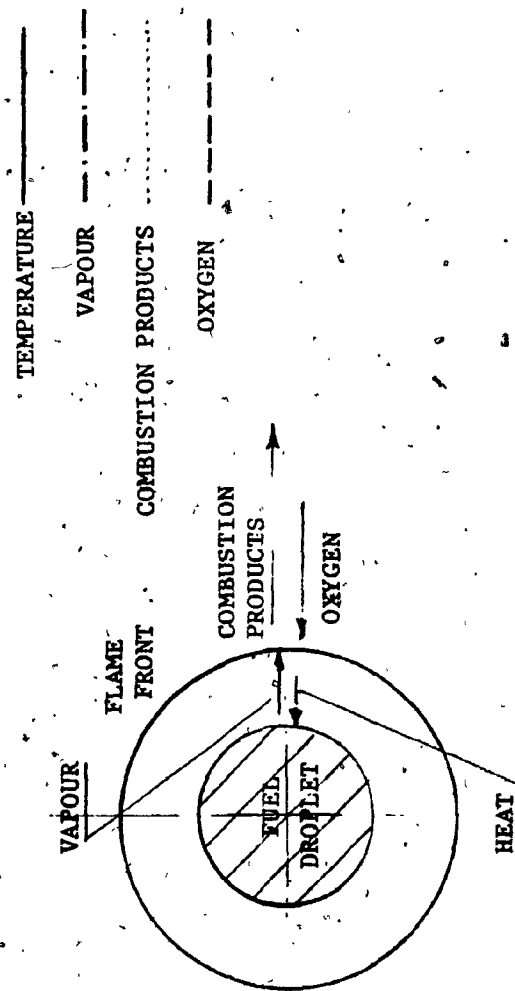
CONSTANTS FOR CALCULATING TOTAL ABSORPTION
OF 1000° C RADIATION BY HEAVY FUEL OIL

FUEL	Gray-Body Absorption Co-efficient K (cm^{-1})	Gray-Plus-Clear Model $\alpha = a (1 - e^{-K'x})$	
		$K' (\text{cm}^{-1})$	$\alpha \text{ cm}^{-1}$
Bunker-C Fuel A	302	38.9	0.88
Bunker-C Fuel B	23.7	45.9	0.71
6 Pure HC's	14.3 - 17.6	28.4 - 29.3	0.61 - 0.73

TABLE 8
VALUE OF "B" IN AIR

FUEL	B
Iso-Octane	6.41
Benzene	5.97
n-Heptane	5.82
Toluene	5.69
Aviation Gasoline	5.51
Automobile Gasoline	5.33
Kerosene	3.42
Gas Oil	2.51
Light Fuel Oil	2.00
Heavy Fuel Oil	1.72

FIGURES



Q_1 = DROP CENTRE
 A_1 = DROP SURFACE
 B_1 = REACTION SURFACE
 C_1 = OUTER EDGE OF STAGNANT FILM

FIG. 1 SPHERICALLY SYMMETRICAL MODEL OF A BURNING DROPLET

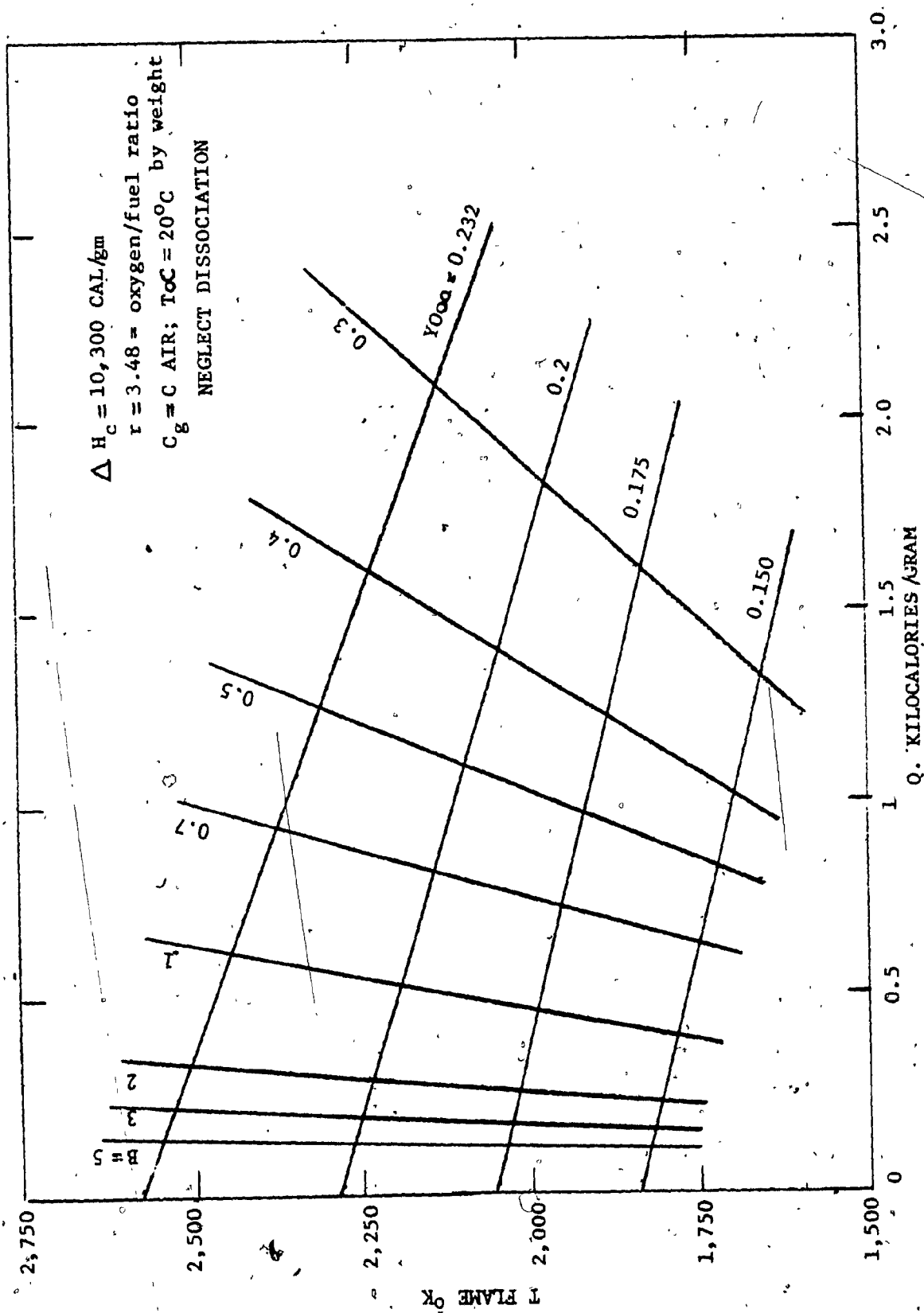


FIG. 2
 FLAME TEMPERATURE FOR VARIOUS
 COMMON HYDROCARBON LIQUID FUEL [82]

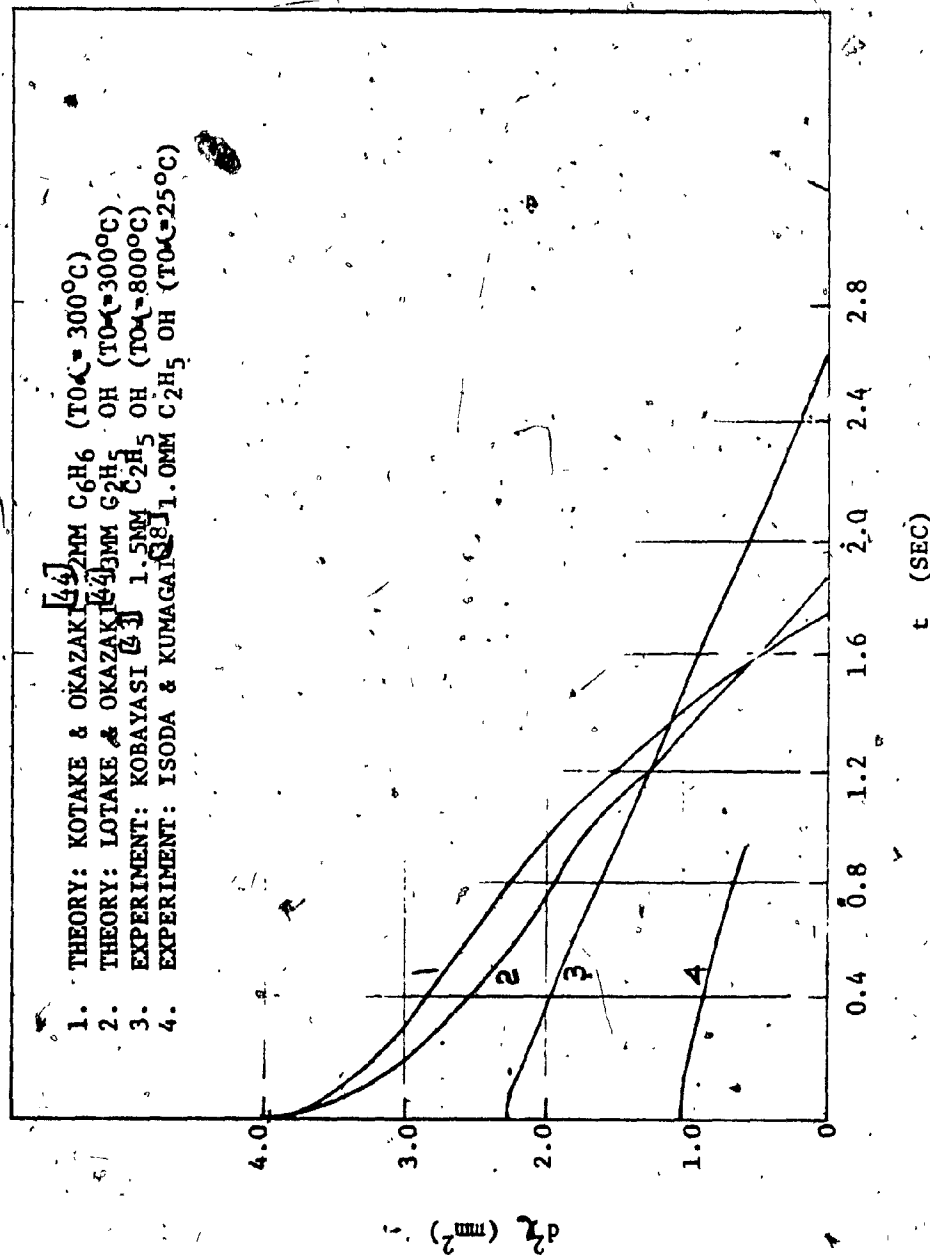


FIG. 3
 COMPARISON OF D_2 AGAINST "t" CURVES IN REF. [44] WITH
 EXPERIMENTAL RESULTS REF [38; 43]

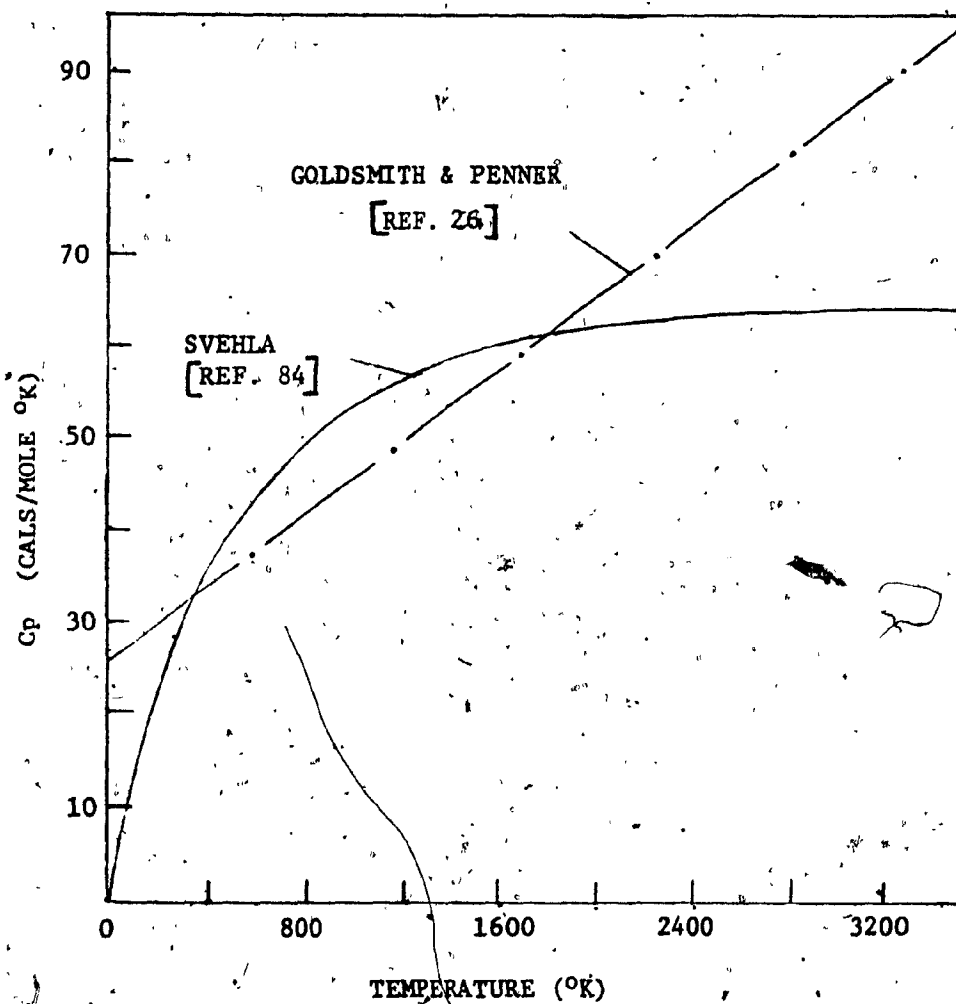


FIG. 4 VARIATION OF SPECIFIC HEAT (C_p) WITH TEMPERATURE FOR BENZENE

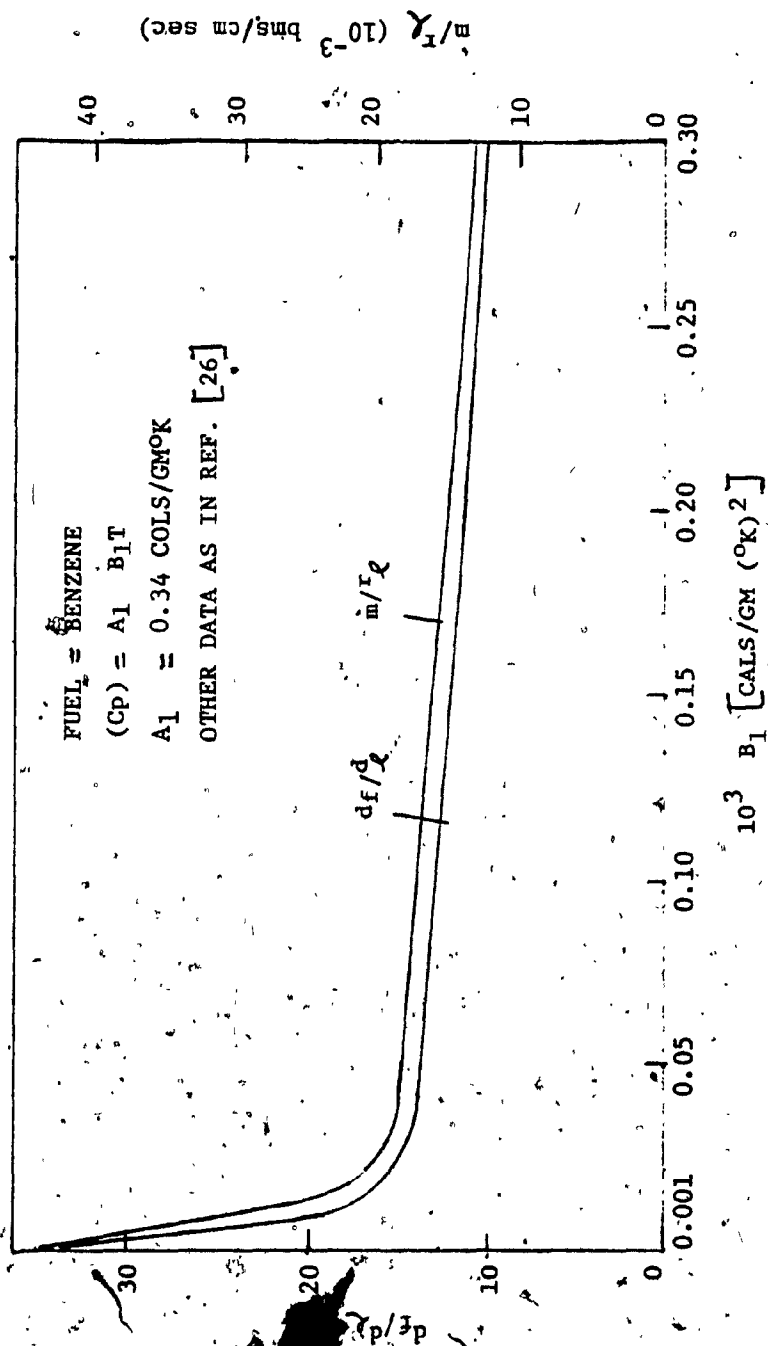


FIG. 5 DEPENDENCE OF $\frac{df}{dT}$ AND $\frac{m}{T}$ ON b_1
 IN THE ANALYSIS OF GOLDSMITH AND PENNER [26]

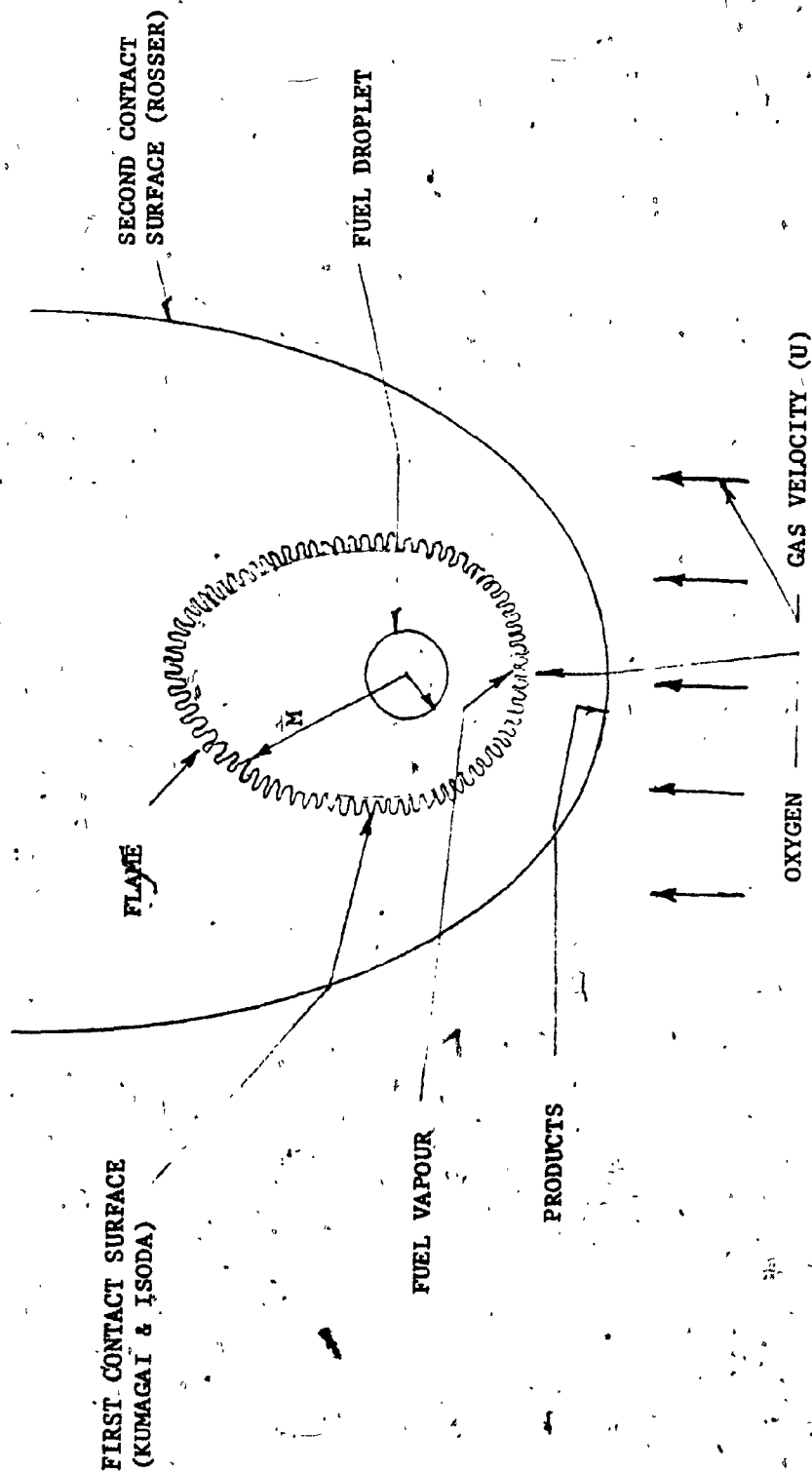
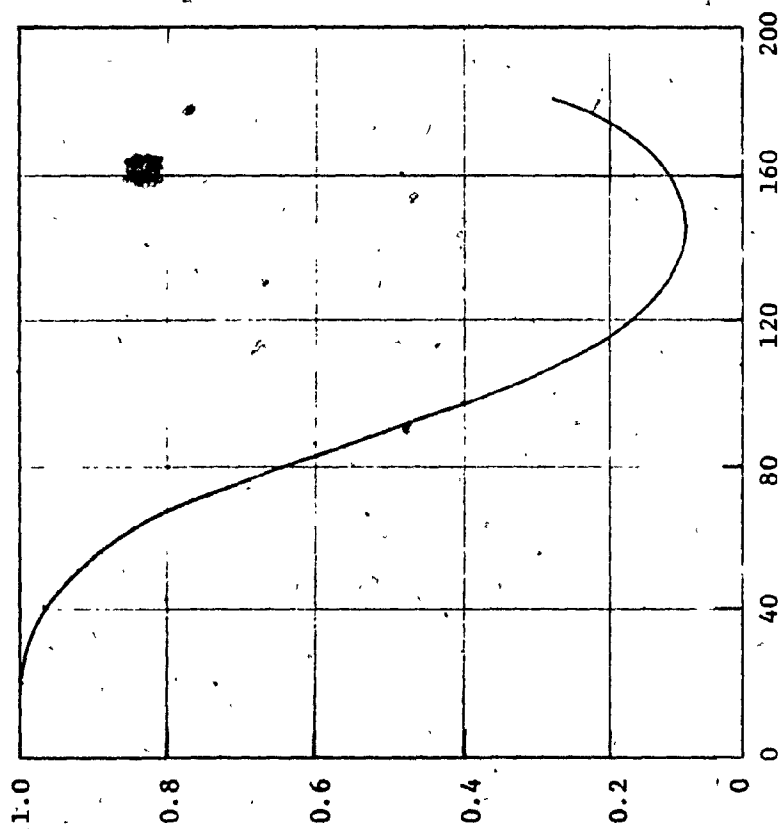


FIG. 6 IDEAL MODEL OF A BURNING DROPLET
IN PRESENCE OF CONVECTION



ANGLE FROM FORWARD STAGNATION POINT, DEG.

($Re \approx 136$)

FIG. 7 THE VARIATION OF LOCAL HEAT TRANSFER RATE OVER A DROP SURFACE UNDER FORCED CONVECTION CONDITIONS (AFTER GRAVES AND Bahr^[2])

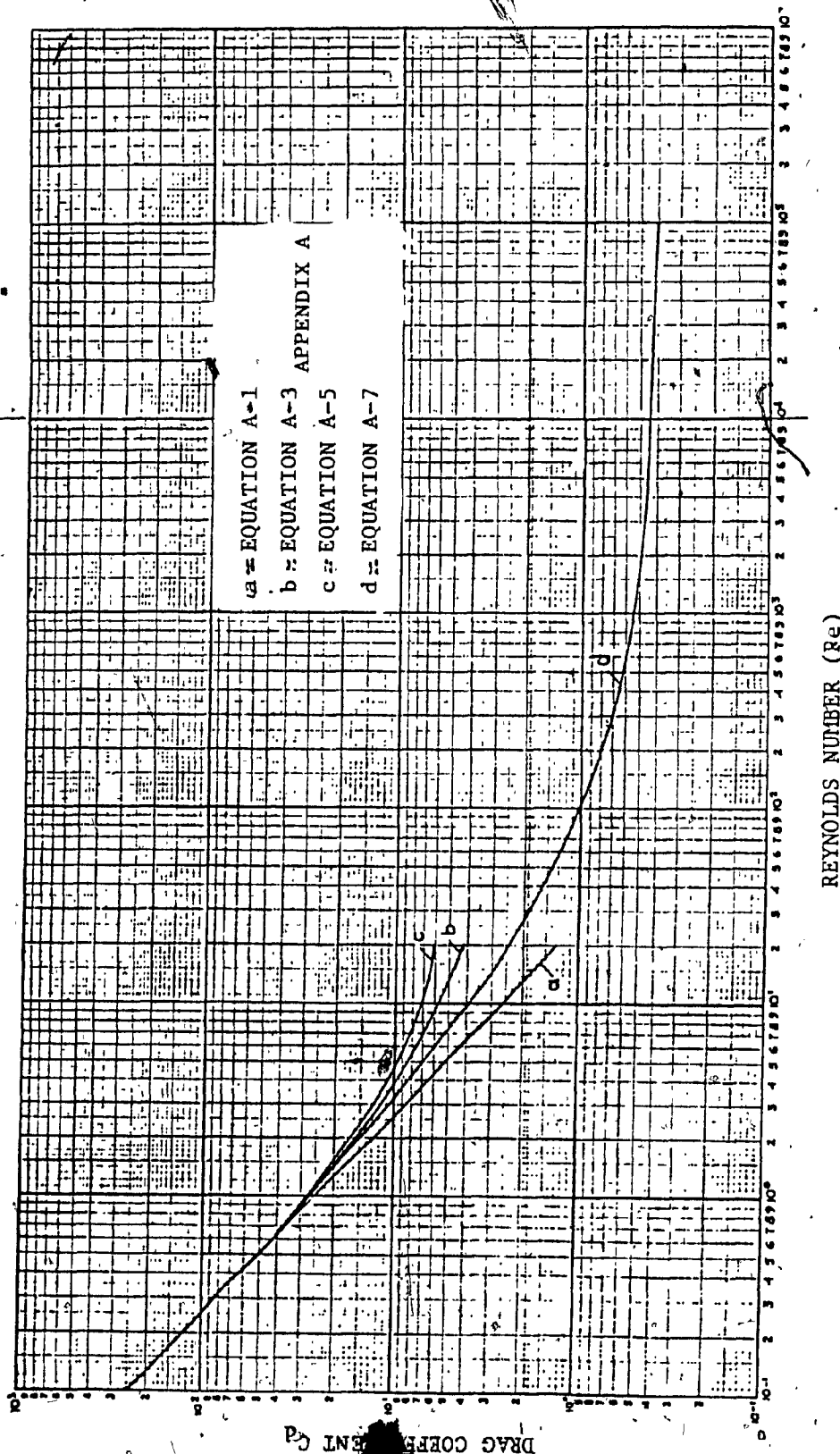
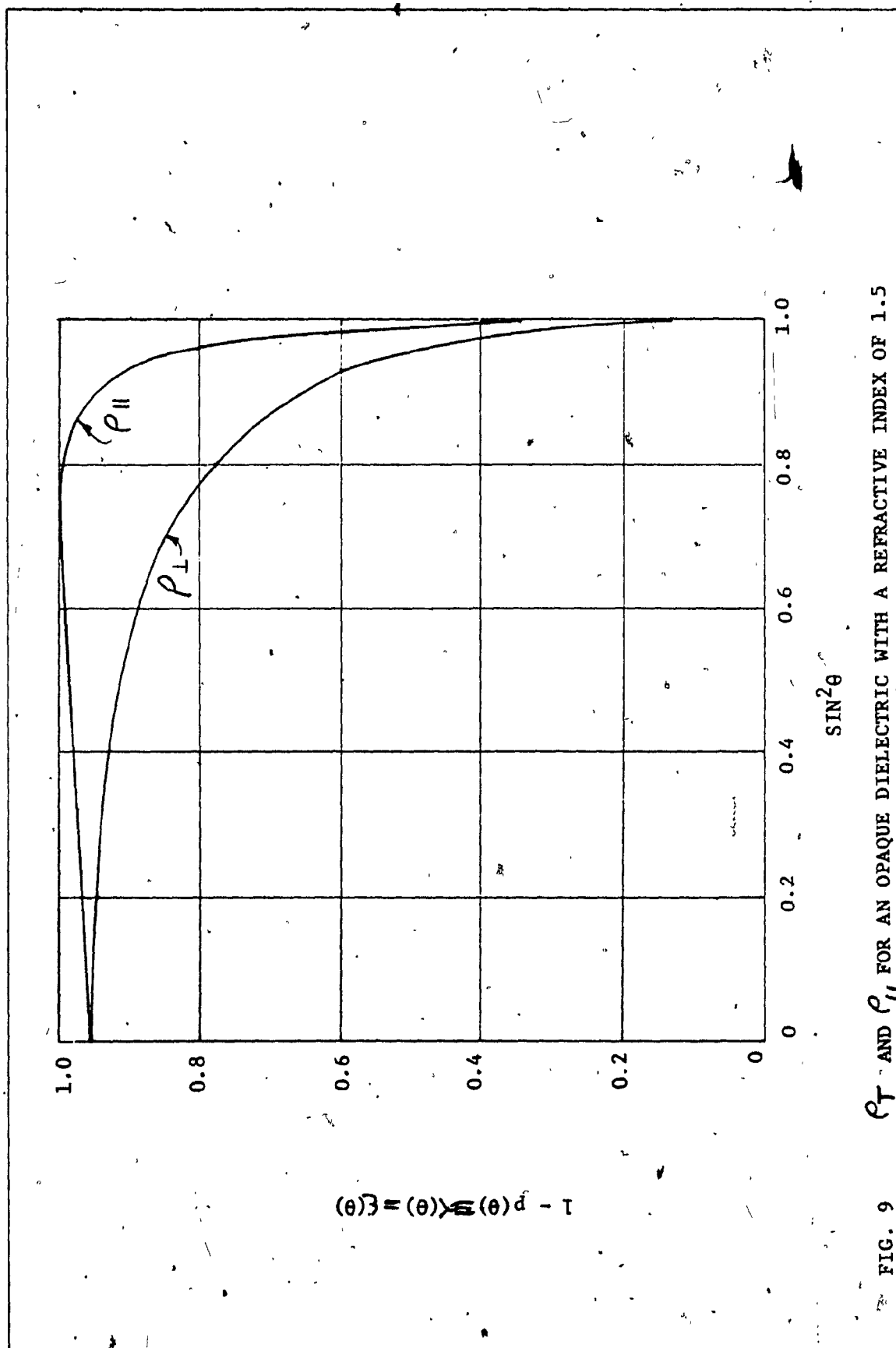


FIG. 8 DRAG COEFFICIENT (C_d) AGAINST REYNOLDS NUMBER (Re) FOR THE COMBUSTION OF A DROPLET IN FORCED CONVECTIVE ATMOSPHERE



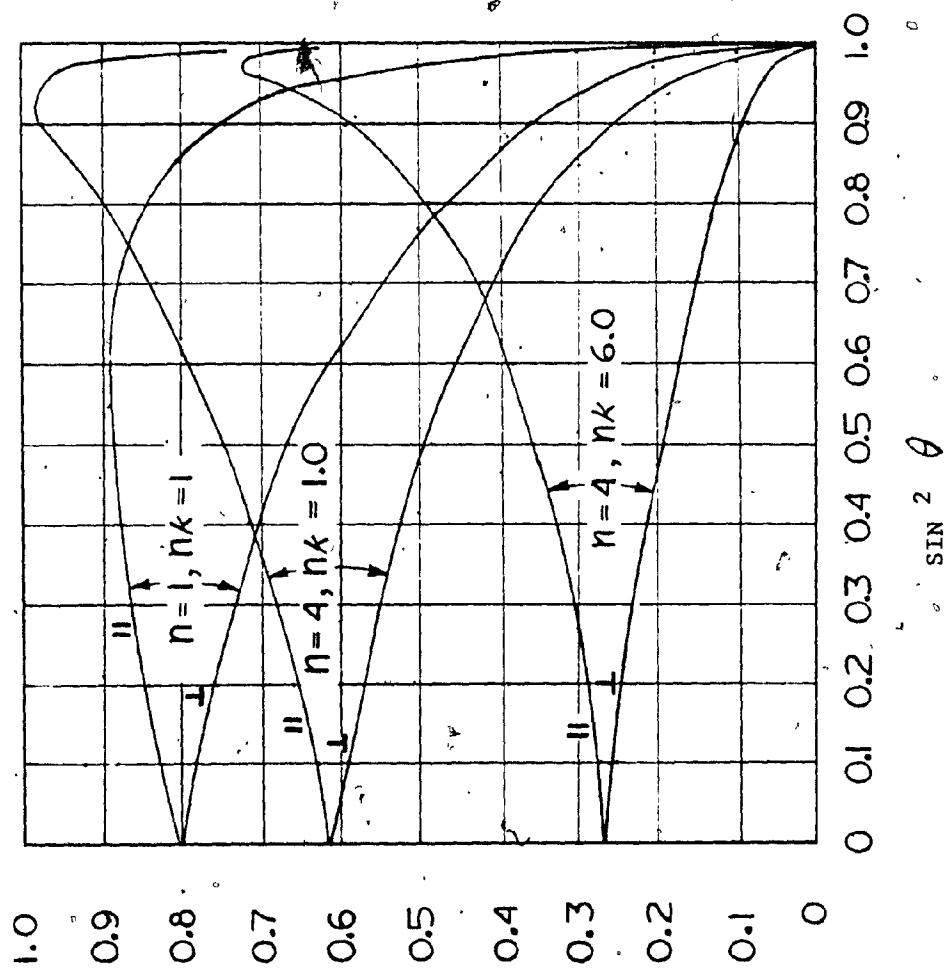


FIG. 10 DIRECTIONAL EMISSIVITY OF STRONG ABSORBERS

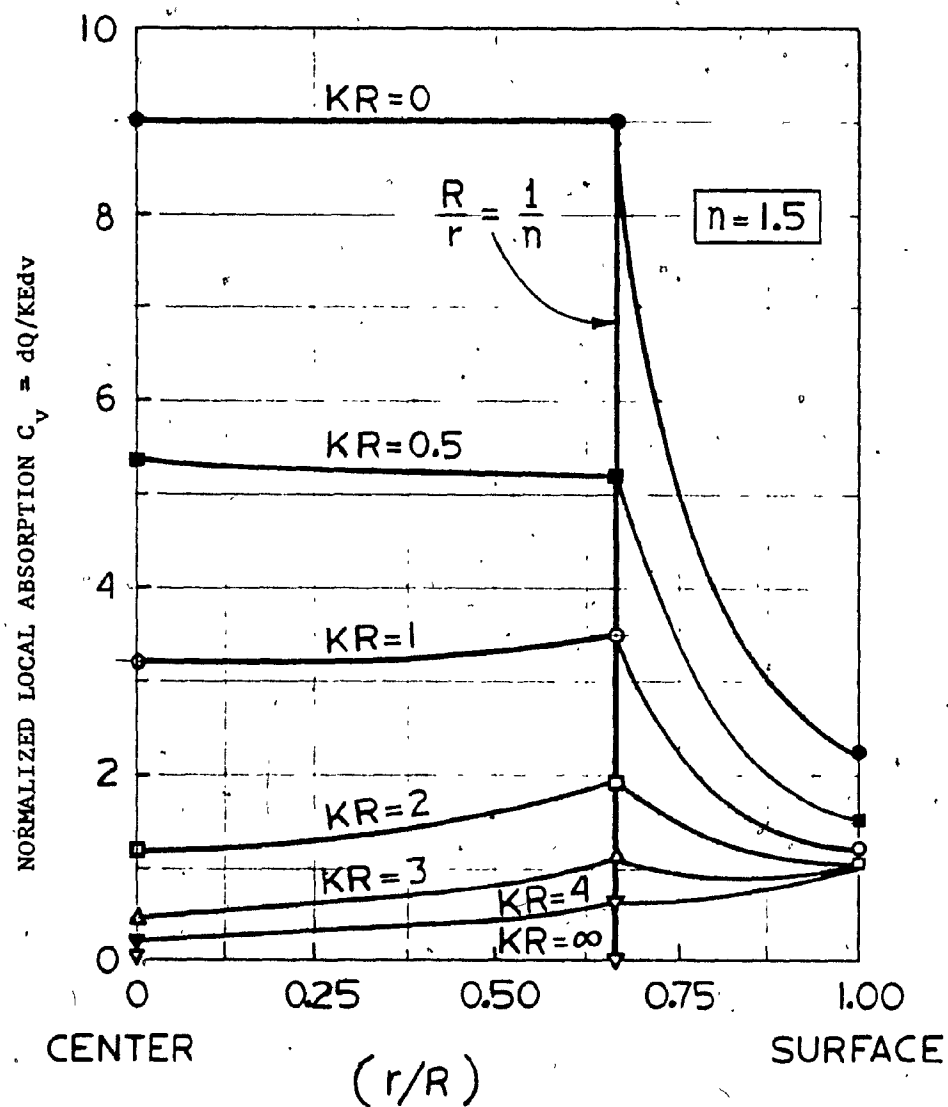


FIG. 11 - INTERNAL LOCAL VOLUMETRIC ABSORPTION RATE IN AN ABSORBING - REFLECTING SPHERE THE SURFACE OF WHICH IS UNIFORMLY IRRADIATED WITH HEMISPHERICAL FLUX; REFRACTIVE INDEX ≈ 1.5

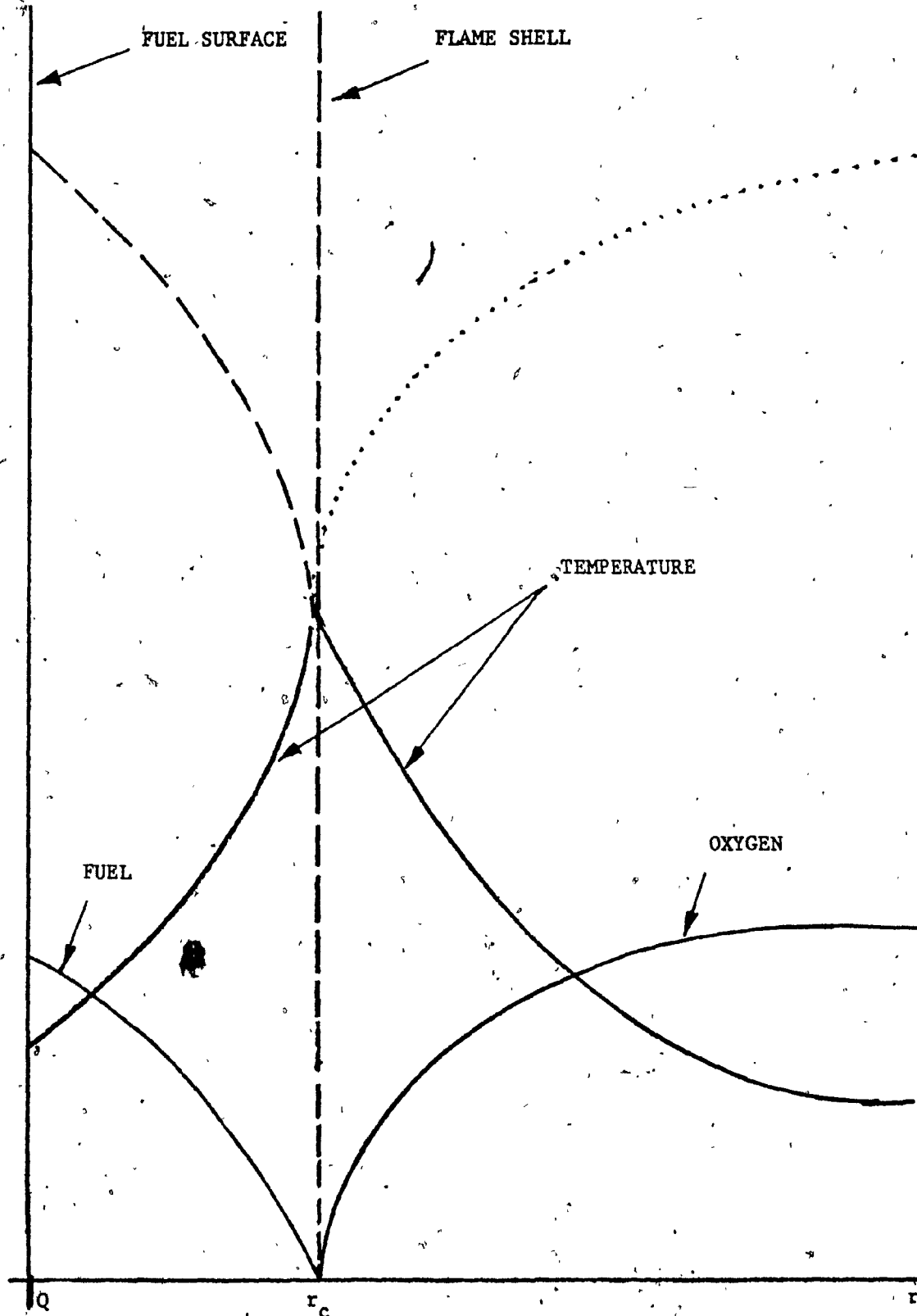


FIG. 12

SPECIES AND TEMPERATURE PROFILE
FOR A BURNING DROPLET

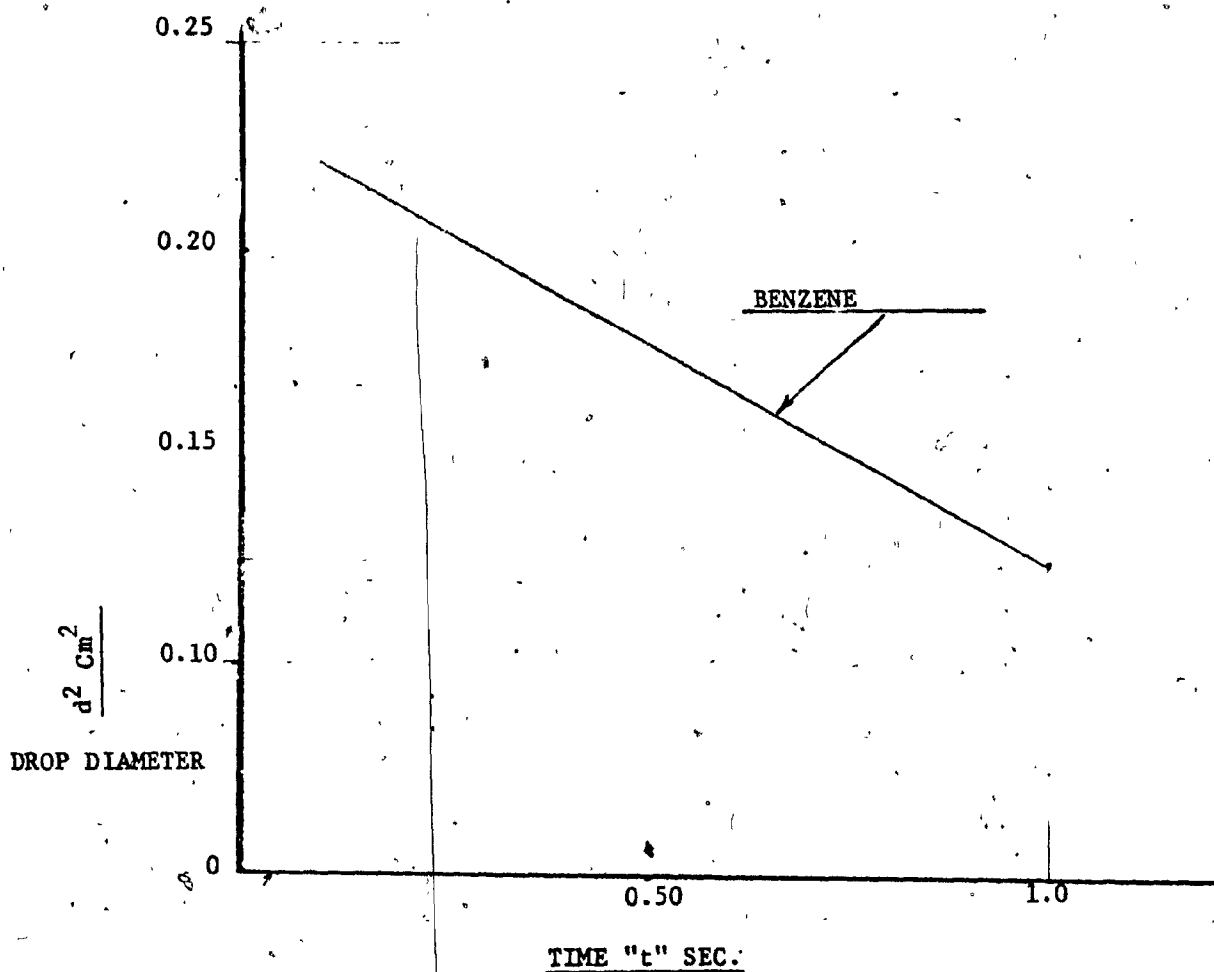


FIG. 13 BENZENE DROPLET IN STAGNANT AIR
SHOWING DIAMETER SQUARED TIME DEPENDENCY [22]

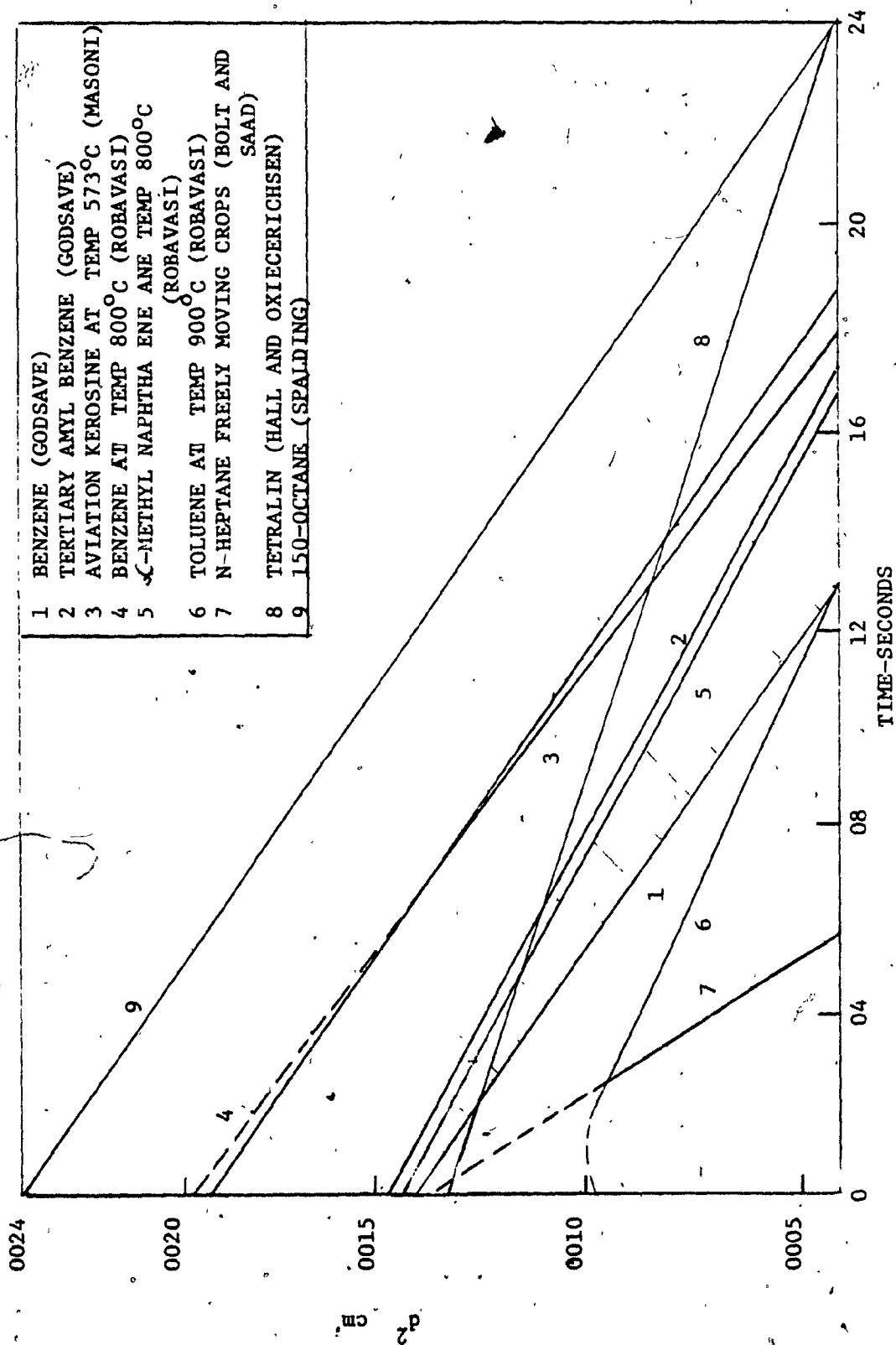


FIG. 14 RELATIONSHIP OF d^2 AGAINST t FOR SINGLE DROPLETS OF VARIOUS FUELS

REFERENCES

REFERENCES

1. Agoston, G.A., Wood, B.J, and wise, M. Jet Propulsion, 1958 28,181.
2. Agoston, G.A. Wise, H., and Rosser, W.A. 6th Symposium (Int.) on combustion. Reinhold, New York, 1957, p. 708.
3. Aldred, J.W. and Williams, A., Combust. Flame 10,396 (1966).
4. Audunson, I., and Gebhart, B., "An experimental and analytical study of Natural Convection with appreciable thermal radiation effects", Journal of Fluid Mechanics, Vol. 52, Part 1, Mar. 1972, pp. 57-95.
5. Beer, J.M., J.Inst, fuel 35.3: 1962
6. B. Brown, A.M. Pressure-jet oil burners for boiler use. Major developments in liquid fuel firing, 1948-1959, Torquay, 11th to 14th May, 1959, Institute of Fuel, 1959.
7. Broeze J.J., G. Riband and D.A. Saunders J. Inst: Fuel 24:51 (1951).
8. Brzustowski, T.A. and Natarajan, R., Can. J. Chem. Eng. 44,194 (1966).
9. Brzustowski T.A., Can. J. Chem. Eng. 1965 43:30.
10. Basset, A.B.A. treatise on Hydrodynamics, Cambridge, 1888.
11. Boussinesq. J. Theorie Analatique de la Chaleur, Paris, 1903. C.

12. Chihier, N.A. in Preprints for the Symposium on Evaporation- combustion of fuel droplets, presented before the Division of Petroleum Chemistry, Inc., American Chemical Society, Aug. 29 - Sept. 3, 1976, Vol. 21, No. 4, p. 616, 1976.
13. Chen, C.M. Mean value and correlation problems connected with the motion of small particles suspended in turbulent fluid. Martinus, Nijhoff, The Hague, 1947.
14. C'Rowe, C.T., Nicholls, J.A. and Morrison, R.B. 9th symposium (Int) on combustion. Academic Press, London, 1963, p. 395.
15. Echigo, R., Nishiwaki, N., and Hirata, M.: Eleventh symposium (International) on combustion, p. 381, The Combustion Institute, 1967.
16. Edwards, D.K., and Menard, W.A., "Comparison of Models for Correlation of Total Band Absorption", Appl. Opt., Vol. 3, No. 5, May 1964, pp. 621-625.
17. Elsasser W.M.: Harvard Meteorological series No. 6, Harvard University, Cambridge, Mass 1942.
18. Eisenkland P. and Arunachalam. s.a., Combustion and Flame 1966 10,171.
19. Elsenkland P., Arunachalam, S.A., and Weston, J.A., 11th symposium on Combustion, The combustion Institute, Pittsburgh, Pennsylvania, 1967, p. 715.
20. Frossling N. Gerland Beitre, Zur Geophysik 1938, 52,170 (Translation N.R.C. 1979).
21. Frossling N. Gerland, Beitre, Geophysik 1937, 51,167 (Translation S.N.C. 1980).

22. Godsave, G.A.E., Fourth Symposium (International) on Combustion Williams and Wilkins, 1953, p. 818.
23. Goldstein, S. Proc. Roy. Soc. (London), 1929, 123A, 225.
24. Gumz, Q. Feuerungstech, 1938, 26, 253; Arch. Gas Warmetech, 1950, 1, 25.
25. Goldsmith, M., and Penner, S.S. California Inst. Tech. Office of Ordnance. Research Tech. Report No. 2, 1953.
26. Goldsmith, M., and Penner, S.S. Jet propulsion, 1954, 24, 245.
27. Goldsmith M., Jet Propulsion, 1956, 26, 172.
28. Gollahalli, S.R. and Brzustowski, T.A.: Fourteenth Symposium (International) on Combustion, p. 1333, The Combustion Institute, 1973.
29. Graves C.C. and Bahr N.A.C.A. Report 1300 1957, p. 21 (chapter 1)
30. Hall, A.R. and Diederischen, J. 4th Symposium (Int.) on combustion. Williams and Wilkins, Baltimore, 1953, p. 837.
31. Hottel, H.C., In 'Heat Transmission', editor, W.H. McAdams, 3rd Edition, Chap. 4, 1954, McGraw-Hill, New York.
32. Hottel, H.C., Williams, G.C. and Simpson, H.C., 5th Symposium (International) on combustion. Reinhold, New York, p. 101, 1953.
33. Hottel, H.C., and A.F. Sarofim, 'Radiative Transfer'. 1967, McGraw-Hill, New York.
34. How, M.E. The influence of turbulence on the burning rate of fuel suspensions J. Inst. Fuel, 1966, 39, 150.

35. Hubbard, G.L., Denny, V.E. and Mills, A.F., Intern J. Heat Mass Transfer 18, 1003 (1975).
36. Hil denbrand, D.L., Whittaker A.G. and Euston, C.B., JPT Propulsion 1958, 28, 194.
37. Isoda, H., and Kumagai, S. 7th Symposium (Int.) on Combustion, Butterworths, London, 1958. p. 523.
38. Isoda, H. and Kumagai, S., Seventh Symposium (International) on Combustion Butterworths, 1959, p. 523.
39. Isoda, H. and Kumagai, S., Sixth Symposium (International) on Combustion Reinhold, 1957, p. 726.
40. Ingebo, R.D., N.A.C.A., T.N. 3265, 1954.
41. Ingebo, R.D., N.A.C.A. T.N. 3762, 1956.
42. Kassoy, D.R. and Williams, F.A., AIAA J. 6, p. 1961, 1968.
43. Kobaysi, K., Fifth Symposium (International) on Combustion p. 594 Reinhold, 1955, p. 141.
44. Kotake, S., and Okazaki, T. Int. J. Heat Mass Transfer, 1969.
45. Kumagai, S., and Isoda, H. Nature, 1960, 166, 111.
46. Kumagai, S., and Isoda, H. 5th Symposium (Int.) on Combustion, Reinhold, New York, 1955, p. 129.
47. Kumagai, S., and Isoda, H. Ibid, 1956, p. 726.
48. Kumagai, S., and Kimura, I. Science of Machine (Japan), 1951, 3, 431.

49. Kumagai, S. 6th Symposium (Int.) on Combustion. Chapman and Hall London 1956, p. 668.
50. Kumagai, S., Sakai, T, and Okafima, S., Thirteenth Symposium (International) on Combustion. The Combustion Institute, 1971, p. 779.
51. Law, C.K., Combust. Flame, 26, 17 (1976).
52. Langmuir, I., and Blodgett, K. A.A.F.T.R. - 5418, 1946.
53. Law, C.K. and Williams, F.A., Combust. Flame 19, 393 (1972).
54. Long V.D. A Simple Theoretical model of droplet combustion J. Inst. Fuel 1964, 37, 522.
55. M. Lorrel, J., Wise, H., and Carr R.E.J., chem. Phys. 1958 25, 325.
56. Masdin E.G., and Thring, M.W. Combustion of single droplets of liquid fuel, J. Inst. Fuel 1962, 35, 251.
57. Mayorcas R., J. Inst. Fuel 25: 515 (1952).
58. Muggia, A. L'Aerotecnica, 1956, 36, 127, (Translation S.N.C. Montreal).
59. Nishiwaki, N. 5th Symposium (Int.) on combustion, Reinhold, New York, 1955, p. 148.
60. Novotny, J.L., "Radiation Interaction in Nongray Boundary Layers" International Journal of Heat and Mass Transfer, Vol. 11, No. 12 Dec. 1968, pp. 1823-1826.

61. Novotny, J.L. Bankston, J.D., and Lloyd, J.R., "Local Nonsimilarity Applied to Free Convection Boundary Layers with Radiation Interaction". Heat transfer with Thermal Control Applications, Progress in Astronautics and Aeronautics, Vol. 39, 1975, pp. 309-330.
62. Okajima, S., and Kumagai., Fifteenth Symposium (International) on Combustion. The Combustion Institute, 1975, p. 401.
63. Okazaki, T., and Gomi, M. J. Japan Soc. mech. Engrs, 1953, 1-6, 19.
64. Otsuka, Y. and Niioka, T., Combust. Flame 21, 163 (1973).
65. Oseen, C.W. Ark. Mat. Astr. F.Y.S., 1910, 6, No. 29.
66. Oseen, C.W. Hydrodynamik, Leipzeig, 1927.
67. Peskin, R.L. Polymeropoulos, C.E. and Yeh P.S., A.I.A.A. 1967, S(No. 12) 2173
68. Peskin, R.L., and Wise, H., A.I.A.A., 1966, 4, (No. 9), p. 1946.
69. Penner, S.S. Chemistry problems in jet propulsion, Pergamon Press, New York, 1967, p. 267.
70. Penner S.S., Chemistry in jet propulsion, Permagon (1957) pp. 276-291.
71. Richardson, J.F., and Zaki, W.N., Trans. Inst. Chem. Engrs. 1954, 32, 35.
72. Ranz, W.E. and Marshall, W.R., Chem. Engr. Progr. 1952, 48, 141, 173.

73. Richardson, J.W., and Zaki, W.N., Chem. Engng. Sci., 1954, 3, 65.
74. Rosser, W.A. combustion and Flame, 1967, 11, (No. 3) 442.
75. Stokes, G.G., Trans. Comb. phil. Soc., 1851, 9, part 2, 51.
76. Schiller, L., and Naumann, A.Z. Ver dent. Ing. 1933, 77, 318
77. Siegel, R., and Howel, J.R., Thermal Radiation Heat Transfer, p. 589, McGraw-Hill, 1973.
78. Spalding, D.B., 4th Symposium (Int.) on combustion, Williams and Wilkins, Baltimore, 1953, p. 847.
79. Spalding D.B., Fuel 1953, 332, 255.
80. Spalding D.B., Ibid, 169.
81. Spalding, D.B. Some fundamentals of combustion, Vol. 2, Butterworths Scientific publications, London, 1955.
82. Spalding, D.B., "The Combustion of Liquid Fuels", Fourth Symposium (International) on Combustion, Williams and Wilkins, 1953, pp. 847-864.
83. Spalding, D.B., Ars J. 29, p. 828, 1959.
84. Svehla R.A., Estimated Viscosities and Thermal conductivities of gasses at High Temperature, NASA TRR 132-1962.
85. Tarifa C.S., Del Notario P.O. and Moreno, F.G. 8th Symposium (Int.) on combustion, Williams and Wilkins 1962, p. 1035.
86. Thring, M.W., J.M. Beer and P.J. Foster: Thirt International, Heat Transfer Conference pp. 101-111, 1966.

87. Tien, C.L., "Thermal Radiation Properties of Gases".
Advances in Heat Transfer, Vol. 5, Academic Press, New York.
1968, pp. 254-324.
88. Waldman, C.H., Fifteenth Symposium (International) on Combustion,
The Combustion Institute, 1975, p. 429.
89. Williams, A., Combust. Flame 21, 1 (1973).
90. Williams A., Oxidation and combustion, Reviews, 1968, 3, No. 1,
1 to 45.
91. Williams, F.A. Combustion and Flame, 1961, 5, 207.
92. Williams, F.A., J. Chem. Phys., 1960, 33, (No. 1), 133.
93. Williams, F.A., Combustion Theory, Addison-Wesley,
94. Wise, H., and Ablow, C.M., J. Chem. Phys., 1957, 27, 389.
95. Wise, H. Lorresl, J. and Wood, B.J., 5th Symposium (Int.) on
Combustion, Reinhold, New York, 1955, p. 132.
96. Wolfhard, H.G., and Parker, W.G., J. Inst. Petrol, 1949, 35, 118.

APPENDIX A

METHODS OF CALCULATING DRAG CO-EFFICIENTS FOR THE COMBUSTION
OF A DROPLET IN FORCED CONVECTIVE EFFECT

APPENDIX A

METHODS OF CALCULATING DRAG CO-EFFICIENTS FOR THE COMBUSTION OF A DROPLET IN FORCED CONVECTIVE EFFECT.

At viscous flow regime with $Re \leq 0.1$, the flow around the sphere has up and down the stream symmetry. For these conditions, Stokes [75.] neglected the inertia terms of Navier-Stokes equations and obtained the following expression of drag:

$$F = 3\pi d \mu V \quad (A.1)$$

where, F = the drag force

d = sphere diameter

V = velocity of the sphere relative to the fluid

μ = viscosity of the fluid

As C_d is defined by the equation,

$$C_d = F / \rho_g V^2 / 2 A.$$

Where, A = projected area of sphere, $\left[\frac{\pi d^2}{4} \right]$ for a sphere
 ρ_g = the density of the ambient gas.

Thus, $C_d = \frac{24}{Re}$, according to Stokes' law (A.2)

At Oseen's flow regime with $0.1 < Re \leq 1$, the flow pattern is no longer symmetric on the upstream and downstream sides of the sphere and the inertia forces become significant. Oseen, [65] however, linearized the Navier-Stokes equation by considering the inertia terms to be important only in the regions of flow far from the sphere. Goldstein [23] solved the Oseen's linearized equation to give the following expression of C_d :

$$C_d = \frac{24}{Re} \left[1 - \frac{3}{16} Re - \frac{19}{1250} Re^2 - \frac{71}{20481} Re^3 \right] \quad (A.3)$$

For $Re > 1$, the inertia forces become significant even in the region close to the sphere. The fluid flow is further complicated by flow separation, appearance of wake behind the sphere and its subsequent detachment at higher Reynolds Numbers. For these conditions, Oseen's approximation becomes invalid. Owing to the complexity of flow and the consequent non-linearity of the Navier-Stokes equations,

APPENDIX A

METHODS OF CALCULATING DRAG CO-EFFICIENTS FOR THE COMBUSTION OF A DROPLET IN FORCED CONVECTIVE EFFECT. (cont'd)

analytical solutions have not been obtained. However, for $Re \leq 80$, a number of numerical solutions [124] of these equations have been found. In addition, several experimental correlations have been obtained between C_d and Re . Some of the more reliable of these are presented below:

- (i) Schiller and Naumann [76]

$$C_d = \frac{24}{Re} \left[1 + 0.15 Re^{0.687} \right] \quad (A.4)$$

for $Re \leq 100$

- (ii) Langmuir and Blodgett [52]

$$C_d = \frac{24}{Re} \left[1 + 0.197 Re^{0.63} + 0.0023 Re^{1.38} \right] \quad (A.5)$$

for $1 \leq Re \leq 100$

- (iii) Gumz [24] and Frossling [21]

$$\frac{1}{F} = \frac{1}{F_s} + \frac{1}{F_n} \quad (A.6)$$

for $0.5 \leq Re \leq 2000$

Where, F = the actual drag force

F_s = the drag force given by Stokes' law.

F_n = The residual drag force found by using the following pseudo-drag values C_d' ;

$$C_d' = 0.08741 \quad \text{for } 0.5 \leq Re \leq 8$$

$$C_d' = 0.3 \quad \text{for } 8 \leq Re \leq 300$$

$$C_d' = 0.28 \quad \text{for } 300 \leq Re \leq 2000$$

- (iv) Zahm

$$C_d = \frac{24}{Re^{0.85}} + 0.48 \quad (A.7)$$

For $Re \leq 200000$

APPENDIX A

METHODS OF CALCULATIONS DRAG CO-EFFICIENTS FOR THE COMBUSTION OF A DROPLET IN FORCED CONVECTIVE EFFECT. (cont'd)

Numerical solutions [10, 11, 66] of the Navier-Stokes' equations for $Re < 1$ show that the drag force on an accelerating sphere is a complex function of Re and the acceleration modulus, $\frac{ad}{V^2}$ (where a = sphere acceleration, d = sphere diameter, V = the velocity of the particle relative to the medium).

Crowe et al. [14] solved the integro-differential form of the tangential equation of motion of a thin boundary layer of a sphere. Their results indicate that for the range $250 < Re < 1600$, acceleration reduces the C_{da} (where C_{da} = drag coefficient of sphere in presence of acceleration). However, for $\frac{ad}{V^2} < 10^{-2}$, C_{da} is insensitive to acceleration effects.

Ingebo [40, 41] while studying the individual droplets and sphere (20 to 120 μm diameter) in sprays and in clouds accelerating from rest to 140 to 160 ft/sec², reported decrease in C_{da} and correlated his results by:

$$C_d = \frac{27}{Re} 0.84 \quad (A.8)$$

Lunnon, However, found that acceleration increases C_{da} of spheres, the magnitude of increase diminishing with increasing Re .

Other workers also suggest an increase in C_{da} due to acceleration, the exact magnitude depending on the flow regime.

The results of Richardson and Zaki [71, 73] suggest that C_d of a particle in a cloud is less than that of an isolated sphere and the extent of reduction is a function of particle concentration.

In addition to the above effects, a number of other factors such as turbulent intensity, particle shape, particle orientation, surface roughness, a finite boundary, medium discontinuity, etc., can affect C_d . There have been several recent reviews on the subject.

APPENDIX A

METHODS OF CALCULATIONS DRAG CO-EFFICIENTS FOR THE COMBUSTION OF A DROPLET IN FORCED CONVECTIVE EFFECT. (cont'd)

The equation of motion of an evaporating drop differs from that of an inert sphere by a term which accounts for the inertial force contributed by the mass flux from the surface of the drop. This affects the drag force on the drop.

Spalding [97] showed that momentum of the effusing vapour alters the velocity profiles within the boundary layer and so leads to the increase in the thickness of this layer. As a result, shear force on the surface of the drop (i.e. frictional drag) is reduced.

In the case of burning drop, due to expansion in the flame, combustion gases fill in the low pressure regions within the wake and thus reduce the form drag [118] (i.e. integral of pressure distribution over the surface of the drop).

Analytical solutions of the Navier-Stokes equations for drops undergoing mass transfer have only been obtained for a number of highly idealized systems at $Re \leq 1$.

Muggia [58] determined theoretically the flow around an evaporating sphere at $Re \leq 1$ by coupling Oseen's linearized form of Navier-Stokes' equations with diffusion equation. Using the assumptions of uniform surroundings, uniform drop temperatures, zero tangential velocity and finite radial velocity at the drop surface, he obtained:

$$C_d = \frac{24}{Re} \left[\frac{2 + B}{\left(2 + \frac{3B}{4} - \frac{3}{16} Re (2 + B) \right)} - \frac{B(4+Re)}{3(2+B)} \right] \quad (A.9)$$

Where, $B = C \frac{(T_g - T_s)}{Q}$

T_g = temperature of the ambient gas

T_s = drop surface temperature

Q = latent heat of vaporization

C = specific heat of gas at constant pressure.

APPENDIX A

METHODS OF CALCULATIONS DRAG CO-EFFICIENTS FOR THE COMBUSTION OF A DROPLET IN FORCED CONVECTIVE EFFECT. (cont'd)

The values of C_d predicted by equation A.9 are considerably lower than those of the standard curve.

Equation A.9 has been found to be valid³ for burning drops at low $Re \leq 1$. For this case, B is defined by equation 11. [14]

Crowe et al. studied analytically the effects of burning on the drag coefficients of accelerating particles at $250 < Re < 1600$ and found a decrease in drag when the ratio of the mass flux from the surface to the mass flux in free stream was greater than 0.025.

To take into account the effect of intense mass transfer on the drag coefficients of flat plates in laminar flow, Spalding proposed the following correlation:

$$\frac{C_d}{C_{d0}} = \frac{\ln(1 + B)}{B} \quad (A.10)$$

Where, C_d = drag coefficient in presence of mass transfer

C_{d0} = standard drag coefficient

Eisenklam et al. [19] investigated the effect of intense mass transfer and flame on the drag coefficients of liquid drops and correlated their results of evaporating and burning drops by:

$$\frac{C_d}{C_{d0}} = \frac{1}{1 + B} \quad (A.11)$$

Where the range of Re was

$0.1 < Re < 3$ for burning drops

$0.1 < Re < 40$ for evaporating drops

C_d = drag coefficients in presence of mass transfer.

Both equations A.10 and A.11 give values of C_d considerably lower than the standard curve.

APPENDIX A

METHODS OF CALCULATIONS DRAG CO-EFFICIENTS FOR THE COMBUSTION OF A DROPLET IN FORCED CONVECTIVE EFFECT. (cont'd)

Ingebo [40,41] found that when evaporating spray droplets and inert solid spheres were accelerated in turbulent air stream at $6 \leq Re \leq 400$, a single correlation was obtained:

$$Cd = \frac{27}{Re^{0.84}} \quad (A.12)$$

The values of Cd obtained from equation A.12 lie below the standard curve.

A number of other workers observed significant reduction in the drag coefficients of evaporating and burning drops.

Fledderman and Hanson investigating the effects of turbulence and relative velocity upon the evaporation of liquid fuel spray observed that Cd values in the range $20 \leq Re \leq 100$ were decreased when the ratio of vapour velocity from the droplet to free stream velocity was as low as 0.08. Clamen and Gauvin while working on the drag coefficients of evaporating spheres in turbulent air stream also observed that the mass transfer reduces the drag coefficients within the range of $2100 \leq Re \leq 29800$.

APPENDIX B

COMPUTER PRINT-OUT OF THE THERMODYNAMIC AND TRANSPORT PROPERTIES FOR BENZENE

FLASH BENZENE			
-----STREAM CONDITION-----			
TEMPERATURE, DEG F	100.00	MC LIQUID	100.00
PRESSURE, PSIA	15.00	DRY VAPO	15.00
-----FLOW - RATES-----			
FLOW RATE, LB/MOLS/HR	10.00		0.0
M LBS/HR	0.781		0.0
COLD LIQ RATE, M GALS/HR	0.106		0.0
HOT LIQUID RATE, GPM	1.81		0.0
HOT VAPOR RATE, M FT3/HR	0.0		0.0
-----CHARACTERIZATION VALUES-----			
MOLECULAR WEIGHT	78.108		0.0
API GRAVITY	28.477		0.0
COLD LIQ DENSITY, LB/GAL	7.365		0.0
WATSON K	9.730		0.0
ACENTRIC FACTOR	0.2125		0.0
-----PHYSICAL PROPERTIES-----			
HOT LIQUID SP. GR.	0.8632		0.0
DENSITY, LB/FT3	53.778		0.0
DENSITY, LB/GAL	7.189		0.0
HOT VAPOR DENSITY, LB/FT3	0.0		0.0
VAPOR COMPRESS. FACTOR	0.0		0.0
-----CRITICAL PROPERTIES-----			
CRITICAL COMPRESSIBILITY	0.2750		0.0
PSEUDOCRITICAL TEMP, DEG F	552.00		0.0
TRUE CRITICAL TEMP, DEG F	552.00		0.0
PSEUDOCRITICAL PRES, PSIA	714.00		0.0
TRUE CRITICAL PRES, PSIA	714.00		0.0
-----THERMAL PROPERTIES-----			
IDEAL GAS SPECIFIC HEAT	0.2640		0.0
IDEAL GAS SPEC HEAT RATIO	1.1066		0.0
-----TRANSPORT PROPERTIES-----			
THER COND, BTU/HR.FT.F	8.026E-02		0.0
VISCOSITY, CENTIPOISE	4.938E-01		0.0
VISCOSITY, CENTISTOKES	5.721E-01		0.0

FLASH BENZENE		HC LIQUID	DRY VAPOR
-----STREAM CONDITION-----			
TEMPERATURE, DEG F	200.00	200.00	200.00
PRESSURE, PSIA	15.00	15.00	15.00
-----FLOW RATES-----			
FLOW RATE, LB-MOLS/HR	0.0	0.0	10.00
FLOW RATE, M LRS/HR	0.0	0.0	0.781
COLD LIQ RATE, M GALS/HR	0.0	0.0	0.106
HOT LIQUID RATE, GPM	0.0	0.0	0.0
HOT VAPOR RATE, M FT3/HR	0.0	0.0	4.616
-----CHARACTERIZATION VALUES-----			
MOLECULAR WEIGHT	0.0	0.0	78.108
API GRAVITY	0.0	0.0	28.477
COLD LIQ DENSITY, LB/GAL	0.0	0.0	7.365
WATSON K	0.0	0.0	9.730
ACENTRIC FACTOR	0.0	0.0	0.2125
-----PHYSICAL PROPERTIES-----			
HOT LIQUID SP. GR.	0.0	0.0	0.0
DENSITY, LB/FT3	0.0	0.0	0.0
DENSITY, LB/GAL	0.0	0.0	0.0
HOT VAPOR DENSITY, LB/FT3	0.0	0.0	0.1692
VAPOR COMPRESS. FACTOR	0.0	0.0	0.9785
-----CRITICAL PROPERTIES-----			
CRITICAL COMPRESSIBILITY	0.0	0.0	0.2750
PSEUDOCRITICAL TEMP, DEG F	0.0	0.0	552.00
TRUE CRITICAL TEMP, DEG F	0.0	0.0	552.00
PSEUDOCRITICAL PRES, PSIA	0.0	0.0	714.00
TRUE CRITICAL PRES, PSIA	0.0	0.0	714.00
-----THERMAL PROPERTIES-----			
IDEAL GAS SPECIFIC HEAT	0.0	0.0	0.3156
IDEAL GAS SPEC HEAT RATIO	0.0	0.0	1.0876
-----TRANSPORT PROPERTIES-----			
THE COND, BTU/HR.FT.F	0.0	0.0	9.112E-03
VISCOSITY, CENTIPOISE	0.0	0.0	9.259E-03
VISCOSITY, CENTISTOKES	0.0	0.0	0.0

FLASH BEN/CNE

HC LIQUID DRY VAPOR

-----STREAM CONDITION-----

TEMPERATURE, DEG F 300.00 300.00
PRESSURE, PSIA 15.00 15.00

-----FLOW RATES-----

FLOW RATE, LB-MOLS/HR 0.0 10.00
M LBS/HR 0.0 0.781
COLD LIQ RATE, M GALS/HR 0.0 0.106HOT LIQUID RATE, GPM 0.0 0.0
HOT VAPOR RATE, M FT3/HR 0.0 5.334

-----CHARACTERIZATION VALUES-----

MOLECULAR WEIGHT 0.0 78.108
API GRAVITY 0.0 28.477
COLD LIQ DENSITY, LB/GAL 0.0 7.365
WATSON K 0.0 9.730
ACENTRIC FACTOR 0.0 0.2125

-----PHYSICAL PROPERTIES-----

HOT LIQUID SP. GR. 0.0 0.0
DENSITY, LB/FT3 0.0 0.0
DENSITY, LB/GAL 0.0 0.0
HOT VAPOR DENSITY, LB/FT3 0.0 0.1464
VAPOR COMPRESS. FACTOR 0.0 0.9817

-----CRITICAL PROPERTIES-----

CRITICAL COMPRESSIBILITY 0.0 0.2750
PSEUDOCRITICAL TEMP, DEG F 0.0 552.00
TRUE CRITICAL TEMP, DEG F 0.0 552.00PSEUDOCRITICAL PRES, PSIA 0.0 714.00
TRUE CRITICAL PRES, PSIA 0.0 714.00

-----THERMAL PROPERTIES-----

IDEAL GAS SPECIFIC HEAT 0.0 0.3616
IDEAL GAS SPEC HEAT RATIO 0.0 1.0756

-----TRANSPORT PROPERTIES-----

THER COND, BTU/HR-FT-F 0.0 1.236E-02

VISCOSITY, CENTIPOISE 0.0 1.075E-02
VISCOSITY, CENTISTOES 0.0 0.0

FLASH BENZENE

HC LIQUID DRY VAPOR

-----STREAM CONDITION-----

TEMPERATURE, DEG F 400.00 400.00
PRESSURE, PSIA 15.00 15.00

-----FLOW RATES-----

FLOW RATE, LB-MOLS/HR 0.0 10.00
M LBS/HR 0.0 0.781

COLD LIQ RATE, M GALS/HR 0.0 0.106

HOT LIQUID RATE, GPM 0.0 0.0

HOT VAPOR RATE, M FT3/HR 0.0 6.063

-----CHARACTERIZATION VALUES-----

MOLECULAR WEIGHT 0.0 78.108

API GRAVITY 0.0 28.477

COLD LIQ DENSITY, LB/GAL 0.0 7.365

WATSON K 0.0 9.730

ACENTRIC FACTOR 0.0 0.2125

-----PHYSICAL PROPERTIES-----

HOT LIQUID SP. GR. 0.0 0.0

DENSITY, LB/FT3 0.0 0.0

DENSITY, LB/GAL 0.0 0.0

HOT VAPOR DENSITY, LB/FT3 0.0 0.1288

VAPOR COMPRESS. FACTOR 0.0 0.9862

-----CRITICAL PROPERTIES-----

CRITICAL COMPRESSIBILITY 0.0 0.2750

PSEUDOCRITICAL TEMP, DEG F 0.0 552.00

TRUE CRITICAL TEMP, DEG F 0.0 552.00

PSEUDOCRITICAL PRES, PSIA 0.0 714.00

TRUE CRITICAL PRES, PSIA 0.0 714.00

-----THERMAL PROPERTIES-----

IDEAL GAS SPECIFIC HEAT 0.0 0.4031

IDEAL GAS SPEC HEAT RATIO 0.0 1.0673

-----TRANSPORT PROPERTIES-----

THER COND, BTU/HR.FT.F 0.0 1.620E-02

VISCOSITY, CENTIPOISE 0.0 1.220E-02

VISCOSITY, CENTISTOKES 0.0 0.0

FLASH RENZENF		HC LIQUID	DRY VAPOR
-----STREAM CONDITION-----			
TEMPERATURE, DEG F		500.00	500.00
PRESSURE, PSIA		15.00	15.00
-----FLOW RATES-----			
FLOW RATE, LB-MOLS/HR		0.0	10.00
M LBS/HR		0.0	0.781
COLD LIQ RATE, M GALS/HR		0.0	0.106
HOT LIQUID RATE, GPM		0.0	0.0
HOT VAPOR RATE, M FT3/HR		0.0	6.795
-----CHARACTERIZATION VALUES-----			
MOLECULAR WEIGHT		0.0	78.108
API GRAVITY		0.0	28.477
COLD LIQ DENSITY, LB/GAL		0.0	7.365
WATSON K		0.0	9.730
ACENTRIC FACTOR		0.0	0.2125
-----PHYSICAL PROPERTIES-----			
HOT LIQUID SP. GR.		0.0	0.0
DENSITY, LB/FT3		0.0	0.0
DENSITY, LB/GAL		0.0	0.0
HOT VAPOR DENSITY, LB/FT3		0.0	0.1150
VAPOR COMPRESS. FACTOR		0.0	0.9900
-----CRITICAL PROPERTIES-----			
CRITICAL COMPRESSIBILITY		0.0	0.2750
PSEUDOCRITICAL TEMP, DEG F		0.0	552.00
TRUE CRITICAL TEMP, DEG F		0.0	552.00
PSEUDOCRITICAL PRES, PSIA		0.0	714.00
TRUE CRITICAL PRES, PSIA		0.0	714.00
-----THERMAL PROPERTIES-----			
IDEAL GAS SPECIFIC HEAT		0.0	0.4406
IDEAL GAS SPEC HEAT RATIO		0.0	1.0612
-----TRANSPORT PROPERTIES-----			
THER COND, BTU/HR.FT.F		0.0	2.062E-02
VISCOSITY, CENTIPOISE		0.0	1.359E-02
VISCOSITY, CENTISTOES		0.0	0.0

FLASH BENZENE		HC LIQUID		DRY VAPOR	
-----STREAM CONDITION-----					
TEMPERATURE, DEG F		600.00		600.00	
PRESSURE, PSIA		15.00		15.00	
-----FLOW RATES-----					
FLOW RATE, LB-MOLS/HR		0.0		10.00	
M LBS/HR		0.0		0.781	
COLD LIQ RATE, M GALS/HR		0.0		0.106	
HOT LIQUID RATE, GPM		0.0		0.0	
HOT VAPOR RATE, M FT3/HR		0.0		7.527	
-----CHARACTERIZATION VALUES-----					
MOLECULAR WEIGHT		0.0		78.108	
API GRAVITY		0.0		28.477	
COLD LIQ DENSITY, LB/GAL		0.0		7.365	
WATSON K		0.0		9.730	
ACENTRIC FACTOR		0.0		0.2125	
-----PHYSICAL PROPERTIES-----					
HOT LIQUID SP. GR.		0.0		0.0	
DENSITY, LB/FT3		0.0		0.0	
DENSITY, LB/GAL		0.0		0.0	
HOT VAPOR DENSITY, LB/FT3		0.0		0.1038	
VAPOR COMPRESS. FACTOR		0.0		0.9932	
-----CRITICAL PROPERTIES-----					
CRITICAL COMPRESSIBILITY		0.0		0.2750	
PSEUDOCRITICAL TEMP, DEG F		0.0		552.00	
TRUE CRITICAL TEMP, DEG F		0.0		552.00	
PSEUDOCRITICAL PRES, PSIA		0.0		714.00	
TRUE CRITICAL PRES, PSIA		0.0		714.00	
-----THERMAL PROPERTIES-----					
IDEAL GAS SPECIFIC HEAT		0.0		0.4746	
IDEAL GAS SPEC HEAT RATIO		0.0		1.0566	
-----TRANSPORT PROPERTIES-----					
THER COND, BTU/HR.-FT.-F		0.0		2.562E-02	
VISCOSITY, CENTIPOISE		0.0		1.493E-02	
VISCOSITY, CENTISTOKES		0.0		0.0	

FLASH BENZENE		HC LIQUID	DRY VAPOR
-----STREAM CONDITION-----			
TEMPERATURE, DEG F	700.00	700.00	700.00
PRESSURE, PSIA	15.00	15.00	15.00
-----FLOW RATES-----			
FLOW RATE, LB-MOLS/HR	0.0	0.0	10.00
FLOW RATE, M LBS/HR	0.0	0.0	0.781
COLD LIQ RATE, M GALS/HR	0.0	0.0	0.106
-----HOT LIQUID RATE, GPM-----			
HOT LIQUID RATE, GPM	0.0	0.0	0.0
HOT VAPOR RATE, M FT3/HR	0.0	0.0	8.253
-----CHARACTERIZATION VALUES-----			
MOLECULAR WEIGHT	0.0	0.0	78.108
API GRAVITY	0.0	0.0	28.477
COLD LIQ DENSITY, LB/GAL	0.0	0.0	7.365
WATSON K	0.0	0.0	9.730
ACENTRIC FACTOR	0.0	0.0	0.2125
-----PHYSICAL PROPERTIES-----			
HOT LIQUID SP. GR.	0.0	0.0	0.0
DENSITY, LB/FT3	0.0	0.0	0.0
DENSITY, LB/GAL	0.0	0.0	0.0
HOT VAPOR DENSITY, LB/FT3	0.0	0.0	0.0946
VAPOR COMPRESS. FACTOR	0.0	0.0	0.9951
-----CRITICAL PROPERTIES-----			
CRITICAL COMPRESSIBILITY	0.0	0.0	0.2750
PSEUDOCRITICAL TEMP, DEG F	0.0	0.0	552.00
TRUE CRITICAL TEMP, DEG F	0.0	0.0	552.00
-----PSEUDOCRITICAL PRES, PSIA-----			
PSEUDOCRITICAL PRES, PSIA	0.0	0.0	714.00
TRUE CRITICAL PRES, PSIA	0.0	0.0	714.00
-----THERMAL PROPERTIES-----			
IDEAL GAS SPECIFIC HEAT	0.0	0.0	0.5053
IDEAL GAS SPEC HEAT RATIO	0.0	0.0	1.0530
-----TRANSPORT PROPERTIES-----			
THER COND, BTU/HR-FT-F	0.0	0.0	3.120E-02
VISCOSITY, CENTIPOISE	0.0	0.0	1.621E-02
VISCOSITY, CENTISTOKES	0.0	0.0	0.0

FLASH BENZENE		HC LIQUID	DRY VAPOR
-----STREAM CONDITION-----			
TEMPERATURE, DEG F	800.00	800.00	800.00
PRESSURE, PSIA	15.00	15.00	15.00
-----FLOW RATES-----			
FLOW RATE, LB.MOLS/HR	0.0	0.0	10.00
M LBS/HR	0.0	0.0	0.781
COLD LIQ RATE, M GALS/HR	0.0	0.0	0.106
HOT LIQUID RATE, GPM	0.0	0.0	0.0
HOT VAPOR RATE, M FT3/HR	0.0	0.0	8.976
-----CHARACTERIZATION VALUES-----			
MOLECULAR WEIGHT	0.0	0.0	78.108
API GRAVITY	0.0	0.0	28.477
COLD LIQ DENSITY, LB/GAL	0.0	0.0	7.365
WATSON K	0.0	0.0	9.730
ACENTRIC FACTOR	0.0	0.0	0.2125
-----PHYSICAL PROPERTIES-----			
HOT LIQUID SP. GR.	0.0	0.0	0.0
DENSITY, LB/FT3	0.0	0.0	0.0
DENSITY, LB/GAL	0.0	0.0	0.0
HOT VAPOR DENSITY, LB/FT3	0.0	0.0	0.0870
VAPOR COMPRESS. FACTOR	0.0	0.0	0.9964
-----CRITICAL PROPERTIES-----			
CRITICAL COMPRESSIBILITY	0.0	0.0	0.2750
PSEUDOCRITICAL TEMP, DEG F	0.0	0.0	552.00
TRUE CRITICAL TEMP, DEG F	0.0	0.0	552.00
PSEUDOCRITICAL PRES, PSIA	0.0	0.0	714.00
TRUE CRITICAL PRES, PSIA	0.0	0.0	714.00
-----THERMAL PROPERTIES-----			
IDEAL GAS SPECIFIC HEAT	0.0	0.0	0.5331
IDEAL GAS SPEC HEAT RATIO	0.0	0.0	1.0501
-----TRANSPORT PROPERTIES-----			
THER COND, BTU/HR.FT.F	0.0	0.0	3.737E-02
VISCOSITY, CENTIPOISE	0.0	0.0	1.744E-02
VISCOSITY, CENTISTOKES	0.0	0.0	0.0

FLASH BENZENE		HC LIQUID	DRY VAPOR
-----STREAM CONDITION-----			
TEMPERATURE, DEG F	900.00	900.00	900.00
PRESSURE, PSIA	15.00	15.00	15.00
-----FLOW RATES-----			
FLOW RATE, LB-MOLS/HR	0.0	0.0	10.00
FLOW RATE, M LBS/HR	0.0	0.0	0.781
COLD LIQ RATE, M GALS/HR	0.0	0.0	0.106
HOT LIQUID RATE, GPM	0.0	0.0	0.0
HOT VAPOR RATE, M FT3/HR	0.0	0.0	9.694
-----CHARACTERIZATION VALUES-----			
MOLECULAR WEIGHT	0.0	0.0	78.108
API GRAVITY	0.0	0.0	28.477
COLD LIQ DENSITY, LB/GAL	0.0	0.0	7.365
WATSON K	0.0	0.0	9.730
ACENTRIC FACTOR	0.0	0.0	0.2125
-----PHYSICAL PROPERTIES-----			
HOT LIQUID SP. GR.	0.0	0.0	0.0
DENSITY, LB/FT3	0.0	0.0	0.0
DENSITY, LB/GAL	0.0	0.0	0.0
HOT VAPOR DENSITY, LB/FT3	0.0	0.0	0.0806
VAPOR COMPRESS. FACTOR	0.0	0.0	0.9969
-----CRITICAL PROPERTIES-----			
CRITICAL COMPRESSIBILITY	0.0	0.0	0.2750
PSEUDOCRITICAL TEMP, DEG F	0.0	0.0	552.00
TRUE CRITICAL TEMP, DEG F	0.0	0.0	552.00
PSEUDOCRITICAL PRES, PSIA	0.0	0.0	714.00
TRUE CRITICAL PRES, PSIA	0.0	0.0	714.00
-----THERMAL PROPERTIES-----			
IDEAL GAS SPECIFIC HEAT	0.0	0.0	0.5582
IDEAL GAS SPEC HEAT RATIO	0.0	0.0	1.0477
-----TRANSPORT PROPERTIES-----			
THER COND, BTU/HR.FT.F	0.0	0.0	4.412E-02
VISCOSITY, CENTIPOISE	0.0	0.0	1.861E-02
VISCOSITY, CENTISTOES	0.0	0.0	0.0

FLASH BENZENE		HC LIQUID	DRY VAPOR
-----STREAM CONDITION-----			
TEMPERATURE, DEG F	1000.00	1000.00	1000.00
PRESSURE, PSIA	15.00	15.00	15.00
-----FLOW RATES-----			
FLOW RATE, LB-MOLS/HR	0.0	0.0	10.00
M LBS/HR	0.0	0.0	0.781
COLD LIQ RATE, M GALS/HR	0.0	0.0	0.106
HOT LIQUID RATE, GPM	0.0	0.0	0.0
HOT VAPOR RATE, M FT3/HR	0.0	0.0	10.414
-----CHARACTERIZATION VALUES-----			
MOLECULAR WEIGHT	0.0	0.0	78.108
API GRAVITY	0.0	0.0	28.477
COLD LIQ DENSITY, LB/GAL	0.0	0.0	7.365
WATSON K	0.0	0.0	9.730
ACENTRIC FACTOR	0.0	0.0	0.2125
-----PHYSICAL PROPERTIES-----			
HOT LIQUID SP. GR.	0.0	0.0	0.0
DENSITY, LB/FT3	0.0	0.0	0.0
DENSITY, LB/GAL	0.0	0.0	0.0
HOT VAPOR DENSITY, LB/FT3	0.0	0.0	0.0750
VAPOR COMPRESS. FACTOR	0.0	0.0	0.9976
-----CRITICAL PROPERTIES-----			
CRITICAL COMPRESSIBILITY	0.0	0.0	0.2750
PSEUDOCRITICAL TEMP, DEG F	0.0	0.0	552.00
TRUE CRITICAL TEMP, DEG F	0.0	0.0	552.00
PSEUDOCRITICAL PRES, PSIA	0.0	0.0	714.00
TRUE CRITICAL PRES, PSIA	0.0	0.0	714.00
-----THERMAL PROPERTIES-----			
IDEAL GAS SPECIFIC HEAT	0.0	0.0	0.5809
IDEAL GAS SPEC HEAT RATIO	0.0	0.0	1.0458
-----TRANSPORT PROPERTIES-----			
THER COND, BTU/HR.FT.F	0.0	0.0	5.146E-02
VISCOSITY, CENTIPOISE	0.0	0.0	1.974E-02
VISCOSITY, CENTISTOKES	0.0	0.0	0.0

FLASH BENZENE		HC LIQUID	DRY VAPOR
---STREAM CONDITION---			
TEMPERATURE, DEG F		1100.00	1100.00
PRESSURE, PSIA		15.00	15.00
---FLOW RATES---			
FLOW RATE, LB.MOLS/HR		0.0	10.00
M.LBS/HR		0.0	0.781
COLD LIQ RATE, M GALS/HR		0.0	0.106
HOT LIQUID RATE, GPM		0.0	0.0
HOT VAPOR RATE, M FT3/HR		0.0	11.134
---CHARACTERIZATION VALUES---			
MOLECULAR WEIGHT		0.0	78.108
API GRAVITY		0.0	28.477
COLD LIQ DENSITY, LB/GAL		0.0	7.365
WATSON K		0.0	9.730
ACENTRIC FACTOR		0.0	0.2125
---PHYSICAL PROPERTIES---			
HOT LIQUID SP. GR.		0.0	0.0
DENSITY, LB/FT3		0.0	0.0
DENSITY, LB/GAL		0.0	0.0
HOT VAPOR DENSITY, LB/FT3		0.0	0.0702
VAPOR COMPRESS. FACTOR		0.0	0.9982
---CRITICAL PROPERTIES---			
CRITICAL COMPRESSIBILITY		0.0	0.2750
PSEUDOCRITICAL TEMP, DEG F		0.0	552.00
TRUE CRITICAL TEMP, DEG F		0.0	552.00
---THERMAL PROPERTIES---			
PSEUDOCRITICAL PRES, PSIA		0.0	714.00
TRUE CRITICAL PRES, PSIA		0.0	714.00
IDEAL GAS SPECIFIC HEAT		0.0	0.6014
IDEAL GAS SPEC HEAT RATIO		0.0	1.0441
---TRANSPORT PROPERTIES---			
THER COND, BTU/HR.FT.F		0.0	5.938E-02
VISCOSITY, CENTIPOISE		0.0	2.082E-02
VISCOSITY, CENTISTOKES		0.0	0.0

FLASH BENZENE		HC LIQUID	DRY VAPOR
-----STREAM CONDITION-----			
TEMPERATURE, DEG F	1200.00	1200.00	1200.00
PRESSURE, PSIA	15.00	15.00	15.00
-----FLOW RATES-----			
FLOW RATE, LB-MOLS/HR	0.0	0.0	10.00
M LBS/HR	0.0	0.0	0.781
COLD LIQ RATE, M GALS/HR	0.0	0.0	0.106
HOT LIQUID RATE, GPM	0.0	0.0	0.0
HOT VAPOR RATE, M FT3/HR	0.0	0.0	11.850
-----CHARACTERIZATION VALUES-----			
MOLECULAR WEIGHT	0.0	0.0	78.108
API GRAVITY	0.0	0.0	28.477
COLD LIQ DENSITY, LB/GAL	0.0	0.0	7.365
WATSON K	0.0	0.0	9.730
ACENTRIC FACTOR	0.0	0.0	0.2125
-----PHYSICAL PROPERTIES-----			
HOT LIQUID SP. GR.	0.0	0.0	0.0
DENSITY, LB/FT3	0.0	0.0	0.0
DENSITY, LB/GAL	0.0	0.0	0.0
HOT VAPOR DENSITY, LB/FT3	0.0	0.0	0.0659
VAPOR COMPRESS. FACTOR	0.0	0.0	0.9984
-----CRITICAL PROPERTIES-----			
CRITICAL COMPRESSIBILITY	0.0	0.0	0.2750
PSEUDOCRITICAL TEMP, DEG F	0.0	0.0	552.00
TRUE CRITICAL TEMP, DEG F	0.0	0.0	552.00
PSEUDOCRITICAL PRES, PSIA	0.0	0.0	714.00
TRUE CRITICAL PRES, PSIA	0.0	0.0	714.00
-----THERMAL PROPERTIES-----			
IDEAL GAS SPECIFIC HEAT	0.0	0.0	0.6199
IDEAL GAS SPEC HEAT RATIO	0.0	0.0	1.0428
-----TRANSPORT PROPERTIES-----			
THER COND, BTU/HR.FT.F	0.0	0.0	6.788E-02
VISCOSITY, CENTIPOISE	0.0	0.0	2.185E-02
VISCOSITY, CENTISTORES	0.0	0.0	0.0

FLASH BENZENE		HC LIQUID	DRY VAPOR
---STREAM CONDITION---			
TEMPERATURE, DEG F		1300.00	1300.00
PRESSURE, PSIA		15.00	15.00
---FLOW RATES---			
FLOW RATE, LB-MOLS/HR		0.0	10.00
FLOW RATE, M LBS/HR		0.0	0.781
COLD LIQ RATE, M GALS/HR		0.0	0.106
HOT LIQUID RATE, GPM		0.0	0.0
HOT VAPOR RATE, M FT3/HR		0.0	12.564
---CHARACTERIZATION VALUES---			
MOLECULAR WEIGHT		0.0	78.108
API GRAVITY		0.0	28.477
COLD LIQ DENSITY, LB/GAL		0.0	7.365
WATSON K		0.0	9.730
ACENTRIC FACTOR		0.0	0.2125
---PHYSICAL PROPERTIES---			
HOT LIQUID SP. GR.		0.0	0.0
DENSITY, LB/FT3		0.0	0.0
DENSITY, LB/GAL		0.0	0.0
HOT VAPOR DENSITY, LB/FT3		0.0	0.0622
VAPOR COMPRESS. FACTOR		0.0	0.9984
---CRITICAL PROPERTIES---			
CRITICAL COMPRESSIBILITY		0.0	0.2750
PSEUDOCRITICAL TEMP, DEG F		0.0	552.00
TRUE CRITICAL TEMP, DEG F		0.0	552.00
PSEUDOCRITICAL PRES, PSIA		0.0	714.00
TRUE CRITICAL PRES, PSIA		0.0	714.00
---THERMAL PROPERTIES---			
IDEAL GAS SPECIFIC HEAT		0.0	0.6365
IDEAL GAS SPEC HEAT RATIO		0.0	1.0416
---TRANSPORT PROPERTIES---			
THER COND, BTU/HR.FT.F		0.0	7.697E-02
VISCOSITY, CENTIPOISE		0.0	2.285E-02
VISCOSITY, CENTISTOKES		0.0	0.0

FLASH BENZENE		HC LIQUID	DRY VAPOR
-----STREAM CONDITION-----			
TEMPERATURE, DEG F	1400.00	1400.00	1400.00
PRESSURE, PSIA	15.00	15.00	15.00
-----FLOW RATES-----			
FLOW RATE, LB-MOLS/HR	0.0	0.0	10.00
M LBS/HR	0.0	0.0	0.781
COLD LIQ RATE, M GALS/HR	0.0	0.0	0.106
HOT LIQUID RATE, GPM	0.0	0.0	0.0
HOT VAPOR RATE, M FT ³ /HR	0.0	0.0	13.283
-----CHARACTERIZATION VALUES-----			
MOLECULAR WEIGHT	0.0	0.0	78.108
API GRAVITY	0.0	0.0	28.477
COLD LIQ DENSITY, LB/GAL	0.0	0.0	7.365
WATSON K	0.0	0.0	9.730
ACENTRIC FACTOR	0.0	0.0	0.2125
-----PHYSICAL PROPERTIES-----			
HOT LIQUID SP. GR.	0.0	0.0	0.0
DENSITY, LB/FT ³	0.0	0.0	0.0
DENSITY, LB/GAL	0.0	0.0	0.0
HOT VAPOR DENSITY, LB/FT ³	0.0	0.0	0.0588
VAPOR COMPRESS. FACTOR	0.0	0.0	0.9987
-----CRITICAL PROPERTIES-----			
CRITICAL COMPRESSIBILITY	0.0	0.0	0.2750
PSEUDOCRITICAL TEMP, DEG F	0.0	0.0	552.00
TRUE CRITICAL TEMP, DEG F	0.0	0.0	552.00
PSEUDOCRITICAL PRES, PSIA	0.0	0.0	714.00
TRUE CRITICAL PRES, PSIA	0.0	0.0	714.00
-----THERMAL PROPERTIES-----			
IDEAL GAS SPECIFIC HEAT	0.0	0.0	0.6516
IDEAL GAS SPEC HEAT RATIO	0.0	0.0	1.0406
-----TRANSPORT PROPERTIES-----			
THER COND, BTU/HR.FT.F	0.0	0.0	8.664E-02
VISCOSITY, CENTIPOISE	0.0	0.0	2.380E-02
VISCOSITY, CENTISTORES	0.0	0.0	0.0

FLASH BENZENE		HC LIQUID	DRY VAPOR
-----STREAM CONDITION-----			
TEMPERATURE, DEG F	1500.00	1500.00	1500.00
PRESSURE, PSIA	15.00	15.00	15.00
-----FLOW RATES-----			
FLOW RATE, LB.MOLS/HR	0.0	0.0	10.00
M LPS/HR	0.0	0.0	0.781
COLD LIQ RATE, M GALS/HR	0.0	0.0	0.106
HOT LIQUID RATE, GPM	0.0	0.0	0.0
HOT VAPOR RATE, M FT3/HR	0.0	0.0	14.003
-----CHARACTERIZATION VALUES-----			
MOLECULAR WEIGHT	0.0	0.0	78.108
API GRAVITY	0.0	0.0	28.477
COLD LIQ DENSITY, LB/GAL	0.0	0.0	7.365
WATSON K	0.0	0.0	9.730
ACENTRIC FACTOR	0.0	0.0	0.2125
-----PHYSICAL PROPERTIES-----			
HOT LIQUID SP. GR.	0.0	0.0	0.0
DENSITY, LB/FT3	0.0	0.0	0.0
DENSITY, LB/GAL	0.0	0.0	0.0
HOT VAPOR DENSITY, LB/FT3	0.0	0.0	0.0558
VAPOR COMPRESS. FACTOR	0.0	0.0	0.9992
-----CRITICAL PROPERTIES-----			
CRITICAL COMPRESSIBILITY	0.0	0.0	0.2750
PSEUDOCRITICAL TEMP, DEG F	0.0	0.0	552.00
TRUE CRITICAL TEMP, DEG F	0.0	0.0	552.00
PSEUDOCRITICAL PRES, PSIA	0.0	0.0	714.00
TRUE CRITICAL PRES, PSIA	0.0	0.0	714.00
-----THERMAL PROPERTIES-----			
IDEAL GAS SPECIFIC HEAT	0.0	0.0	0.6652
IDEAL GAS SPEC HEAT RATIO	0.0	0.0	1.0397
-----TRANSPORT PROPERTIES-----			
THER COND, BTU/HR.FT.F	0.0	0.0	9.689E-02
VISCOSITY, CENTIPOISE	0.0	0.0	2.471E-02
VISCOSITY, CENTISTOKES	0.0	0.0	0.0

RUN DATE: 12/80

TIME: 57011

RUN DATE: 12/80

[illegible]

FLASH BENZENE

[illegible]